

1
2
3
4
5
6
7
8
9
10
11
12
13
14
15
16
17
18
19
20
21

Implications of error-prone long-read whole-genome shotgun sequencing on characterizing reference microbiomes

Yu Hu^{1,*}, Li Fang^{1,*}, Christopher Nicholson^{1,2}, Kai Wang^{1,3, §}

1. Raymond G. Perelman Center for Cellular and Molecular Therapeutics, Children's Hospital of Philadelphia, Philadelphia, PA 19104

2. Department of Biology, University of Pennsylvania, Philadelphia, PA 19104

3. Department of Pathology and Laboratory Medicine, University of Pennsylvania, Philadelphia, PA 19104

* These authors contributed equally to this work

§ Correspondence to: wangk@email.chop.edu

Keywords: metagenomics, long-read sequencing, microbiome

22 **Abstract**

23 Single-molecule long-read sequencing technologies, such as Nanopore and PacBio, may
24 be particularly relevant for microbiome studies, since they can perform sequencing
25 without PCR amplification or bacteria culture, and the much longer reads may facilitate
26 assignments of operational taxonomic units (OTUs) from genus to species level.
27 However, due to the relatively high per-base error rates (~15%), the application of long-
28 read sequencing on microbiomes remains largely unexplored, and there is a lack of
29 benchmarking study on reference materials to assess their potential utility in microbiome
30 studies. Here we deeply sequenced two human microbiota mock community samples
31 from the Human Microbiome Project (525x coverage on HM-276D with 20 evenly mixed
32 strains, 1068x coverage on HM-277D with 20 unevenly mixed strains). We showed that
33 assembly programs consistently achieved high accuracy (~99%) and completeness
34 (~99%) for bacterial strains with adequate coverage (~99% in 276D and ~72% in 277D).
35 For HM-277D, we also found that long-read sequencing provides accurate estimates of
36 species-level abundance ($R=0.94$, for 20 bacteria with abundance ranging from 0.005%
37 to 64%). Taxonomic binning and profiling were more accurate at higher rank, while
38 performance decreased at the species level. We further compared the results with data
39 generated from the Illumina short-read sequencing and PacBio long-read sequencing.
40 Our results demonstrate the feasibility to characterize complete microbial genomes and
41 populations from error-prone Nanopore sequencing data, but also highlight necessary
42 bioinformatics improvements for future metagenomics tool development. All the data sets
43 on reference microbiomes are made publicly available to facilitate benchmarking studies
44 on metagenomics and the development of novel software tools.

45 **Background**

46 The fundamental importance of microbiota as the microbial communities that reside in
47 human body is increasingly recognized. Over the past decade, there have been
48 tremendous amounts of evidence suggesting that microbiota plays a crucial role in human
49 health through modulating the metabolic functions, as well as food energy harvest and
50 storage. Microbiota, especially the gut microbiota, is associated with many chronic
51 diseases such as obesity, diabetes, metabolic syndrome, inflammatory bowel disease
52 (IBD), irritable bowel syndrome (IBS), liver disease, hepatocellular and colorectal
53 carcinoma[1-14]. Therefore, accurate profiling of complete genomes and population are
54 crucial to understanding the impact of microbiota on human health. Currently, high-
55 throughput sequencing technologies have been widely used in microbial community
56 characterization. In particular, 16S ribosomal RNA (rRNA)[15] and shotgun metagenome
57 sequencing on Illumina platforms[16] are two dominant approaches for describing
58 microbiomes. Overall, the high-throughput nature of metagenomics sequencing allows us
59 to interpret microbial community by using computational approaches such as operational
60 taxonomic unit (OTU) identification[17], abundance quantification[18], read assembly[19-
61 23], binning and taxonomic profiling[24-29]. Specifically, 16S rRNA sequencing targets
62 on very specific regions that are highly variable between species, which is much cost-
63 efficient. This is very useful for us to examine and compare the microbiota across high
64 number of samples in a large scale project. However, this technique can only identify
65 bacteria but not viruses or fungi, and the low resolution limits its usage in microbiome
66 study below the genus level. As opposed to only the 16S sequences, shotgun
67 metagenome sequencing surveys the whole genomes of all organism in the community

68 [30-32]. It allows us to perform deep investigation of the microbial community as its ability
69 to capture sequences from all organisms.

70 Despite the theoretical advantage of shotgun metagenome sequencing, due to the short
71 read length (150 to 300 nucleotides), metagenomes cannot be fully characterized by next-
72 generation sequencing (NGS) data. In addition, the lack of contextual information has
73 become a barrier for short read to span both intra- and intergenomic repeats, which is
74 crucial for complete de novo genome assembly of all dominant species in a microbial
75 community. As a consequence, short-read assemblies remain highly fragmented. In
76 comparison, the use of long-read sequencing has the potential to facilitate the complete
77 and contiguous metagenome assembly. Lee *et al.* [33] sequenced a reference mock
78 community sample using PacBio long read and evaluated the metagenome assembly
79 performance. Results showed that single-molecule real-time (SMRT) long read data
80 offered significantly improved assembly contiguity by spanning many of repetitive regions
81 while single bacteria chromosome was assembled to more than 50 contigs based on short
82 read data. In recent years, the Oxford Nanopore technologies (ONT) have offered
83 advantages over traditional short-read NGS technologies in genome study. This single-
84 molecule sequencing platform is able to generate average read length of >10kbp,
85 spanning low complexity and repetitive genomic regions, which provides much more
86 continuous assemblies. Subsequently, this approach has become an attractive option in
87 metagenomics sequencing. While the ONT have great potential, complete and
88 contiguous de novo metagenome assembly is still constrained by the high error rate
89 (~15%) of single-molecule long-read sequence data[34]. Therefore, a comprehensive
90 evaluation of long-read bioinformatics tools in microbial profiling is needed[35]. Nicholls

91 *et al.*[36] presented Nanopore sequencing data sets of two mock communities with 10
92 microbial species from ZymoBIOMICS[37]. They showed the utility of these data sets for
93 future bioinformatics method development for long-read metagenomics. However,
94 publicly available data sets based other sequencing technologies of these samples are
95 limited as the samples are only commercially available and are not well studied so far by
96 competing approaches. A study to evaluate the advantages of Nanopore sequencing in
97 complete microbial genomes and a comparison over other sequencing technologies is
98 still lacking so far.

99 In this article, we generated two deeply sequenced Nanopore data sets from new
100 reference samples that are more commonly studied, and performed comprehensive
101 analysis to compare microbial community profiling performance with PacBio and Illumina
102 technologies. We first generated 525x coverage data on HM-276D mock community
103 sample from Human Microbiome Project, which is an evenly mixed DNA sample of 20
104 bacterial strains (each with 5% abundance). We performed de novo assembly analysis
105 with 4 long-read assemblers at different depth of coverage. 20 bacterial genomes were
106 assembled with high accuracy and genome completeness. This sample also has been
107 well studied by many groups. As mentioned above, Lee et al. [33] sequenced this mock
108 community with PacBio to show the improvement of long-read data in metagenome
109 assembly analysis. Jones *et al.*[5] compared the influence of different NGS platforms on
110 genomic and functional predictions using HM-276D sample. We downloaded these two
111 data sets and compared the performance with Nanopore data. Our results show that
112 Nanopore consistently improved assembly contiguity, and completeness compared to
113 PacBio and Illumina across computational approaches. Next, we sequenced HM-277D

114 Mock Community sample with 1068x coverage. HM-277D is unevenly mixed DNA sample
115 of 20 bacterial strains. Kuleshove *et al.*[38] sequenced this sample with Illumina TruSeq
116 synthetic long read technique and showed the improvement in bacterial species
117 identification, genome reconstruction compared to short sequences. Also, Leggett *et al.*
118 [39] demonstrated Nanopore metagenomics sequence can be reliably classified using
119 this community. In addition to metagenome assembly, we evaluated taxonomy binning
120 and profiling performance across technologies (Nanopore and PacBio) and samples (HM-
121 276D and HM-277D). High identification and classification accuracy were achieved above
122 the species level. Overall, we demonstrate the technical feasibility to characterize
123 complete microbial genomes and populations from error-prone Nanopore sequencing
124 without any DNA amplification. We also discuss the limitations of current bioinformatics
125 tools, when dealing with error-prone long-read metagenomics sequencing data. All our
126 data are made publicly available, to benefit computational tool development on long-read
127 based microbial genome assembly for metagenomics studies.

128 **Results**

129 **Sequence data quality**

130 HM-276D DNA sample includes 20 evenly mixed bacteria strains with reference genome
131 size 70 Mb in total with 39 chromosomes. 11,610,183 reads with 35,578,375,166 bases
132 (525x coverage depth) were generated on the Nanopore GridION platform, with a median
133 length of 1,374 bp. The N50 length is 6,828 bp and median read quality is 9.39 in Phred
134 scale. By using minimap2, 95% of reads were successfully aligned to reference genomes
135 of 20 bacterial strains with 13.1% error rate. As shown in **Figure 1(a)**, read coverage

136 across 20 bacterial strains has good agreement with known abundances. Read depth is
137 relatively homogenous across bacteria strains with 521.9X (sd = 524.7X) in average.
138 Sequencing depth of each strain is at least 150 reads and only 0.03% region is covered
139 by less than 3 reads.

140

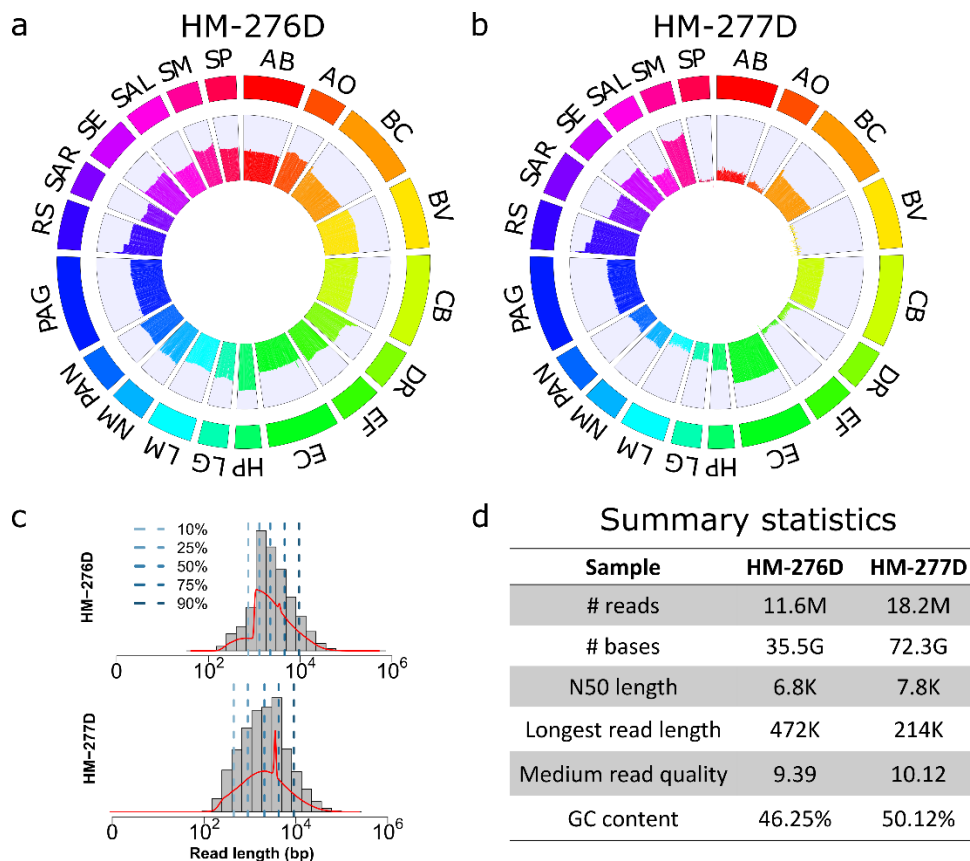
Mapping statistics	HM-276D	HM-277D
# of reads	8,086,684	18,254,839
# of mapped reads	7,640,934	18,110,317
reads unmapped	445,750	144,522
reads MQ0	60,972	103,601
non-primary alignments	287,369	732,671
total length	33,563,573,383	72,312,638,112
bases mapped	32,143,689,158	72,216,146,980
bases mapped (cigar)	31,156,025,998	70,073,211,829
mismatches	4,104,593,752	6,925,222,080
average length	4,150	3,961
maximum length	472,762	214,792
average Phred quality per base	13	17

141

142 **Table 1. Mapping statistics of HM-276D and HM-277D sequenced data set.**
143 Sequenced data were mapped against reference genomes of 20 known bacterial strains.
144 Sequences indicates the number of QC passed reads. Number of mapped and unmapped
145 reads were summarized. MQ0 represents number of mapped reads with MQ=0. Clipping
146 was ignored when calculating total length, bases mapped. Bases mapped (cigar) provides

147 a more accurate number of mapped bases. Number of mismatches were obtained from
 148 NM field of BAM file.

149 HM-277D DNA sample includes 20 unevenly mixed bacteria strains. 18,254,839 reads
 150 data set with 72,312,638,112 bases (1068x coverage depth) were generated, leading to
 151 2,065 bp in median read length with 10.12 median read quality. The N50 length is 7,857
 152 bp. 99.2% of QC-passed reads were mapped to the reference genome and the error rate
 153 was 9.8%. As shown in **Figure1(b)**, read distribution is more heterogeneous across
 154 strains due to unevenly mixed samples. The average coverage is 988.8 reads with
 155 standard deviation =1941.6 bp. This leads to 1.6% of region with less than 3 reads
 156 covered and 4 strains with sequencing depth less than 10 bp, which makes it more difficult
 157 for biological interpretation of this microbial community.

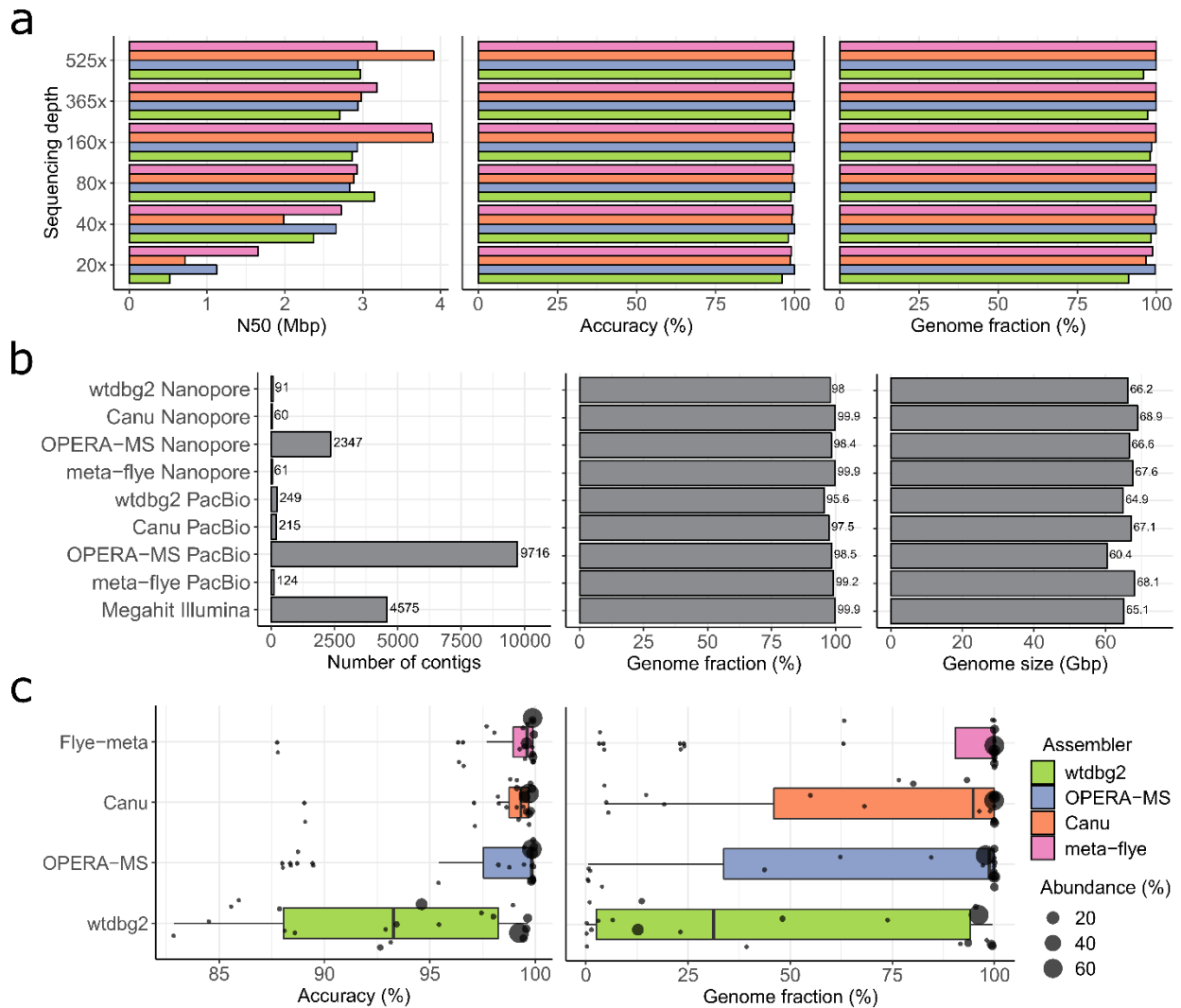


159 **Figure 1. Summary of Nanopore Sequencing data from HM-276D and HM-277D**
160 **microbial communities. (a, b)** Circos plots of read coverage across whole genome of
161 20 bacterial strains from **(a)** HM-276D and **(b)** HM-277D. Each chromosome was divided
162 to bins with 5,000 bp width. Average read coverage was calculated within each bin and
163 converted to log scale to facilitate viewing and comparing between bacterial strains. AB,
164 *Acinetobacter baumannii*; AO, *Actinomyces odontolyticus*; BC, *Bacillus cereus*; BV,
165 *Bacteroides vulgatus*; CB, *Clostridium beijerinckii*; DR, *Deinococcus radiodurans*; DF,
166 *Enterococcus faecalis*; EC, *Escherichia coli*; HP, *Helicobacter pylori*; LG, *Lactobacillus*
167 *gasseri*; LM, *Listeria monocytogenes*; NM, *Neisseria meningitides*; PAN,
168 *Propionibacterium acnes*; PAG, *Pseudomonas aeruginosa*; RS, *Rhodobacter*
169 *sphaeroides*; SAR, *Staphylococcus aureus*; SE, *Staphylococcus epidermidis*; SAL,
170 *Streptococcus agalactiae*; SM, *Streptococcus mutans*; SP, *Streptococcus pneumoniae*; **(c)**
171 Read length distribution of HM-276D and HM-277D data sets. Blue dashed lines
172 represent different quantiles. Red line represents the density of read length distribution.
173 **(d)** Summary statistics of HM-276D and HM-277D data sets. Each value was calculated
174 by using pycoQC [40] and LongreadQC

175 ***De novo* assembly of HM-276D mock community**

176 To assess the ability of Nanopore sequencing in profiling microbial community, we first
177 conducted a de novo assembly of data set with 525x coverage from HM-276D mock
178 community using 4 assemblers: wtdbg2[19], OPERA-MS[20], Canu[21] and meta-
179 flye[22]. Canu and meta-flye are designed to be capable of handling metagenome data,
180 while wtdbg2 and canu are broadly used for haploid or diploid genomes. Overall, the
181 results show promise for the characterization of microbial genomes using long-read
182 sequencing data. Canu produced the largest assembly of 69.5 Mb (99.3% of the
183 benchmark data), including 83 contigs with contig N50 length of 3.91 Mb. meta-flye
184 assembled 67.7Mb genome with 89 contigs. wtdbg2 generated similar results with 64.9

185 Mb genome size, 61 contigs and 2.97 Mb N50 length. Assembly metrics of OPERA-MS
186 (67.9 Mb genome size, 4734 contigs with contig N50 length of 2.94 Mb) are similar with
187 Canu and wtdbg2 whereas much more contigs were generated because OPERA-MS
188 utilizes both long and short sequencing reads for assembly. By mapping all contigs to the
189 reference genomes using MUMMer v3.23, we assessed the accuracy and genome
190 completeness of contigs produced by 4 assemblers. As shown in **Figure 2(a)**, meta-flye
191 achieved the highest genome fraction (99.99%) and 1-to-1 identity percentage (99.62%),
192 followed by OPERA-MS (genome fraction: 99.98% and accuracy 99.92%), Canu
193 (genome fraction 99.81% and accuracy 99.4%) and wtdbg2 (genome fraction 95.94%
194 and accuracy 98.73%). Thus, 4 tools generated results with similar good quality in term
195 of contiguity, accuracy and completeness using long read data with evenly mixed samples
196 at 525x coverage depth.



197

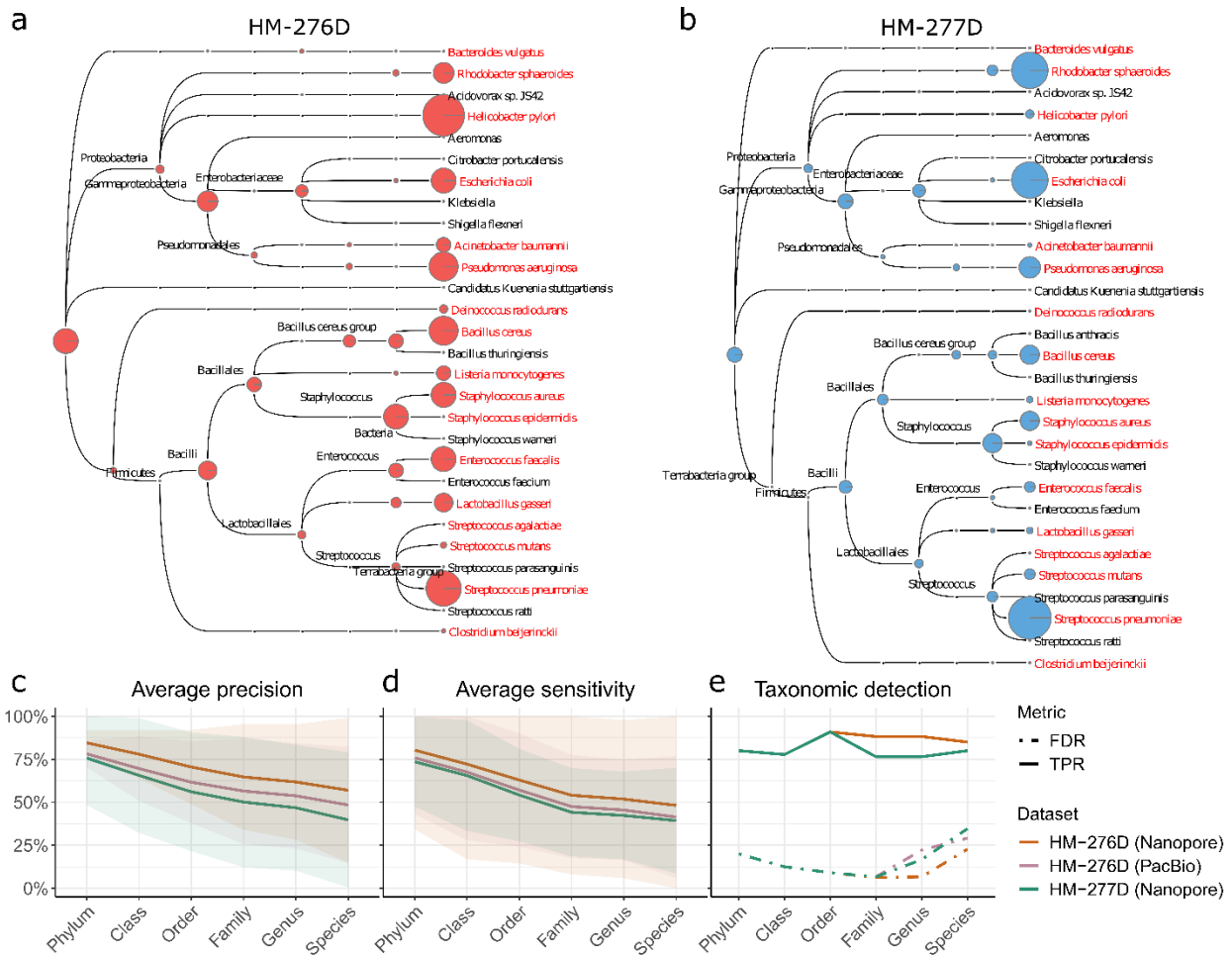
198 **Figure 2. Assembly results for HM-276D and HM-277D data sets. (a)** Assembly
 199 statistics (N50 length, accuracy and genome fraction) of each assembler at different
 200 coverage depths based on HM-276D data set. Colors indicate results from different
 201 assemblers (See **Supplementary material** for details in parameter settings). **(b)**
 202 Assembly statistics (number of contigs, genome fraction and genome size) of each
 203 assembler based on HM-276D sample sequenced by different technologies (Nanopore,
 204 PacBio, Illumina). To make fair comparison, each data set was down-sampled to 160x
 205 depth of coverage. **(c)** Strain-specific assembly performance of each assembler based
 206 on HM-277D data set. Assembly statistics (accuracy and genome fraction) distributions
 207 were presented using boxplots with jitter. Radius of each dot indicates the known relative
 208 abundance of each bacteria strain from the mock community.

209 Next, we subsampled 525× data set to 365× (70%), 160× (30%), 80× (15%), 40× (7.5%)
210 and 20× (3.75%) to examine the effect of sequencing depths on de novo assembly. The
211 assembly results of 4 tools ranges 95.95% to 99.96% in consensus accuracy and 91.26%
212 to 99.99% in genome fraction. In specific, OPERA-MS outperforms others with the highest
213 and most consistent metrics for completeness and accuracy across different sequencing
214 depths because its metagenomics design substantially improves the robustness to low
215 sequencing depth, where genome fractions are 99.68% in average (sd = 0.61%) and
216 consensus identities are 99.92% in average (sd = 0.05%). Despite of reduced metrics as
217 sequencing depth becoming lower, meta-flye and Canu still recovered at least 96.8%
218 genomes with 98.5% accuracy. Notably, wtdbg2 improved the assembly metrics with
219 coverage depth reduced from 520× to 80×. In addition, we examined whether genomes
220 of 20 bacterial strains can be better constructed with Nanopore sequencing technology
221 compared to PacBio and Illumina. As shown in **Figure 2(b)**, assemblers using Nanopore
222 sequenced data outperforms other two technologies. With the same assembler, on
223 average, the number of contigs of Nanopore is ~30% lower than PacBio, genome fraction
224 and genome size are 1.56% and 3.1 Mb higher respectively. Assemblies using Illumina
225 sequenced data are 99.9% in accuracy, but with more contigs generated and lower
226 genome size in total compared to Nanopore.

227 ***De novo* assembly of HM-277D mock community**

228 To evaluate the metagenome reconstruction in a more realistic setting, we carried out
229 another de novo assembly of 1068× data set from HM-277D Mock Community, with
230 unevenly mixed DNA samples of the 20 bacteria strains. Assembly accuracy still remains

231 high, ranging from 97.78% to 99.75% across tools. However, not surprisingly, genome
232 fractions and genome sizes of all methods are substantially lower than even community.
233 This is because 13 bacterial strains have extremely low abundances (<1%) in this
234 unevenly mixed samples, leading to reduced genome coverage fractions (Canu: 71.68%,
235 OPERA-MS: 71.25%, meta-flye: 91.57%, wtdbg2: 59.7%) and genome sizes (Canu:
236 50.21 Mb, OPERA-MS: 47.99 Mb, meta-flye: 64.12 Mb, wtdbg2: 41.85 Mb). To assess
237 how strain abundance affects assemblies, we calculated strain-specific genome fraction
238 for each tool in **Figure 2(a)**. Across bacterial strains, meta-flye recovered the highest
239 percentage of genome (median 100%), followed by OPERA-MS (median: 98.75%) and
240 Canu (median 94.78%), while assemblies of wtdbg2 covered only 31.22% (median). For
241 bacteria with relative abundance higher than 0.2%, least 99.99% of reference genome
242 can be covered by assembly contigs (meta-flye), with identity consensus reaching to
243 99.93%. These results suggest that bacterial strain with nontrivial abundance can be
244 accurately assembled with Nanopore sequenced data. Overall, we observed that meta-
245 flye returned assemblies for 20 bacterial strains with the best performance in
246 completeness and accuracy. Metric for each strain is correlated with abundance of the
247 corresponding bacteria. Some strains were proved hard to assemble for all assemblers
248 due to extremely low relative abundance. For example, 13.6% of region of *Enterococcus*
249 *faecalis* (0.011% relative abundance) were covered by 0 or 1 read and 56.1% covered by
250 less than 3 reads, leading to 4.47% genome fraction for meta-flye. Moreover, there were
251 2 contigs belong to two different bacteria species, *Bacteroides vulgatus* (0.19% relative
252 abundance) and *Streptococcus pneumoniae* (0.05% relative abundance), indicating the
253 difficulty in differentiating one bacteria from another with low relative abundance.



254

255 **Figure 3. Taxonomic binning results for HM-276D and HM-277D data sets. (a,b)**
 256 Megan taxonomic tree assignment obtained from HM-276D **(a)** and HM-277D **(b)**
 257 Nanopore sequenced data sets. Both data sets were downsampled to 160x depth of
 258 coverage. Each read was aligned against NCBI-nr protein reference data base, then
 259 binned and visualized using Megan-LR. Megan taxonomic tree showing bacteria taxa
 260 identified and their corresponding abundances across taxonomic rank. The radius of
 261 circle represents the number of reads assigned for each taxa. Bacterial strains highlighted
 262 in red represent true organisms in the mock community. **(c-e)** Taxonomic binning and
 263 identification performance metrics across ranks based on different data sets (indicated by
 264 colors). Average **(c)** precision and **(e)** sensitivity and their 95% CIs were calculated based
 265 on metrics from different taxon at each rank. **(e)** Taxonomic detection accuracy metrics,
 266 true positive rate (solid) and false positive rate (dashed), were calculated based on

267 identified taxon (reads > 10) at each rank. To make fair comparison, each data set was
268 downsampled to 160x depth of coverage.

269

270 **Taxon binning and identification**

271 Metagenome assemblers construct contigs with variable length to recover original
272 genome of each bacteria from microbial community. Subsequently, another major
273 challenge in studying the identity and diversity of this community member is to classify
274 sequenced reads or contigs correctly according to their taxonomic origins. Here we
275 investigated the taxonomic binning performance based on 3 scenarios of long-read
276 sequencing data, HM-276D (Nanopore, PacBio) and HM-277D (Nanopore) at 160x depth
277 of coverage, using a state-of-art taxonomic binner Megan-LR. First, all long reads were
278 aligned to NCBI-nr database. Then, we used Megan-LR with interval-union LCA algorithm
279 to assign ~2 million aligned reads (~4.6 Mb bases) to taxonomic nodes (**Figure 3(a,b)**).
280 Overall, 4.22 Mb (0.087%) from Nanopore data of HM-276D sample were mis-assigned,
281 while 4.37 Mb (0.075%) and 4.66 Mb (0.141%) for Nanopore data of HM-277D and
282 PacBio data of HM-276D respectively. Specifically, we evaluated the recovery of taxon
283 bins at different ranks. We considered two metrics to quantify the read assignment
284 accuracy, average precision and sensitivity of 20 bacteria strains. For each taxonomic
285 bin, we obtained precision by calculating the percentage of reads correctly classified out
286 of all binned reads. Sensitivity is the percentage of correctly assigned reads out of all
287 reads originally from the bin. As shown in **Figure 3(c)**, HM-276D (Nanopore) has the
288 highest precision, which are all above 60% from phylum to genus. HM-277D (Nanopore)

289 followed, with all above 50%, while HM-276D (PacBio) has the lowest average precision
290 due to predicted small false positive bins at the species level. Sensitivity has similar
291 pattern (**Figure 3(d)**). HM-276D (Nanopore) still appears to be the best data set for read
292 classification than other two and the difference in accuracy between these 3 scenarios is
293 similar across ranks. Nanopore is ~8% higher than PacBio and HM-276D is 10% higher
294 than HM-277D. To evaluate the stability of read assignment accuracy, we calculated 95%
295 confidence interval of precision and sensitivity for each scenario at each rank. Not
296 surprisingly, confidence bands are narrower at higher rank, indicating that more taxon
297 recovery accuracy can be reached. Owing to unevenly mixed bacteria strains, sensitivity
298 is much more variable for HM-277D than other HM-276D. Overall, these results
299 demonstrated the advantage of long-read data in accurate taxon recovery above the
300 family level, while binning accuracy and stability were relatively at the species level.

301 In addition to assigning sequence fragments (reads or contigs) to taxon bins, we
302 recognized the importance of accurate determination of taxonomic identity presence or
303 absence from microbial community. Therefore, we continued to investigate the
304 performance of taxonomic identity prediction between data from HM-276D (Nanopore,
305 PacBio) and HM-277D (Nanopore). For taxon prediction, we defined that the species is
306 significantly present in the community when at least 10 reads were assigned to it, while
307 identity with less than 10 supporting reads was marked as absence. We considered two other
308 metrics to quantify the detection accuracy, true positive rate (TPR) and false discovery rate
309 (FDR), where TPR is the percentage of correctly predicted taxonomic identities out of
310 known existing taxon and FDR is the percentage of incorrectly predicted taxonomic
311 identities out of all predicted taxon. TPR and FDR were calculated at different ranks in

312 **Figure 3(e)**. TPR were consistent across 3 data sets from phylum to order level (90%-
313 77%). Below the order level, PacBio (HM-276D) and Nanopore (HM-277D) are 22% lower
314 compared to Nanopore (HM-276D) (92%-87%). From phylum to family level, FDRs were
315 controlled under 15% for all 3 data sets. However, at the genus level, more than 20% of
316 detections are false for PacBio (HM-276D) and Nanopore (HM-277D) while 6% for
317 Nanopore (HM-276). All 3 scenarios have inflated FDR (>20%) at the species level.
318 Across data sets, there was drastic increase in FDR between phylum to family level and
319 below family level, $10\% \pm 3\%$ and $21\% \pm 5\%$. Similar to binning results, Nanopore data of
320 HM-276D still consistently performed better than other two data sets across ranks.
321 However, accurately predicting taxonomic profiles at the species level still remains
322 challenging due to many false predicted taxonomic identities with 10 to 100 reads
323 assigned incorrectly.

324 **Strain profiling**

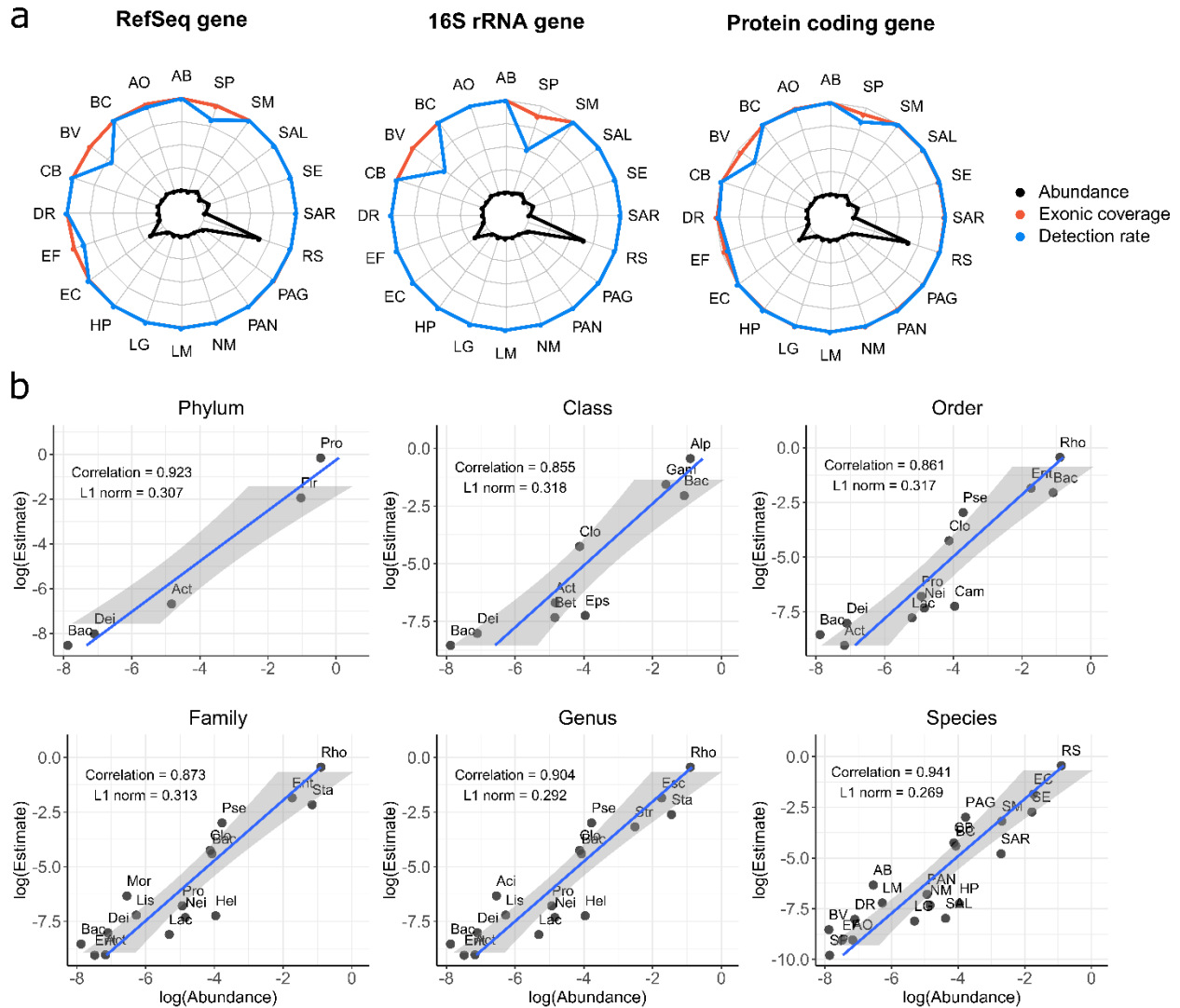
325 Despite the challenges in assembly and binning of HM-277D microbial community even
326 at the species level, especially for low abundance bacteria (relative abundance < 1%),
327 the golden standard profile of this mock community still allows us to evaluate other unique
328 advantages of this deeply sequenced data set at strain level. First, we examined the ability
329 in identifying these 13 extremely rare strains based on annotated target genes. To explore
330 the sensitivity of strain detection using this data set, we mapped raw sequenced reads to
331 reference genomes of the 20 bacterial strains with Minimap2. Then, for each strain-
332 specific gene, the average coverage were estimated by summing up read depth across
333 all exonic region, normalized for gene length. In addition, exon coverage fractions were

334 calculated. We required a gene with average coverage greater than 1 and exon coverage
335 fraction greater 50% simultaneously in order to be declared as a detected gene. The
336 results are shown in **Figure 4(a)**. Detection rates and average coverage among all genes
337 largely keep high in abundant strains (>1%), ranging from 96.4 bp to 4207.6 bp, as well
338 as most of rare strains (<1%). Most of bacterial strains except for *Bacteroides vulgatus*
339 (69.1%) and *Streptococcus pneumoniae* (81.7%) have achieved at least 97% gene
340 detection rate.

341 Next, we recognized that 16S rRNA genes are most commonly used as gene marker for
342 bacteria identification, we further selected them out for each strain based RefSeq
343 annotation. As shown in **Figure 4(a)**, though *Bacteroides vulgatus* and *Streptococcus*
344 *pneumoniae* still have about 50% of 16S rRNA genes undetected by raw sequenced
345 reads, 18 strains have 100% detection rates and exon coverage fraction with 434.77 bp
346 coverage in average, which demonstrates the feasibility of identifying rare strain (<1%) in
347 microbial community with long-read sequencing data. Additionally, read coverage of
348 protein coding genes for 20 bacterial strains was summarized, which shows similar
349 results. 14 strains have average coverage above 100 bp and gene detection rates for 18
350 strains have reached to 99%, indicating the presence of bacterial strains in the sample.

351 To understand the composition, diversity and spatial dynamics of microbial communities,
352 we continued to evaluate the bacterial abundance estimation accuracy based on
353 Nanopore data. We determined two abundance metrics to measure the accuracy,
354 Pearson correlation and L1 norm. These two metrics assess how well Nanopore
355 sequenced reads can reconstruct the bacterial abundances in comparison to the gold

356 standard. Relative abundance was obtained by normalizing total read coverage with
357 chromosome length for each taxon at different ranks. As shown in **Figure 4(b)**,
358 abundance estimates at the species level agrees well with the known relative abundances
359 from the mock community. However, abundance estimation at higher ranks appears to
360 be more challenging, as correlation coefficient ranges from 0.87 to 0.85 and L1 norm is
361 above 0.3 from class to family level, while two metrics improved with Pearson correlation
362 > 0.9 and $L1 < 0.29$ when rank is below the family level. Poor abundance estimation at
363 class or family level may due to the presence of extremely rare bacterial strains in the
364 HM-277D sample, as read coverages were simply summed up between species
365 belonging to the same family or class without accounting for abundance heterogeneity.



366

367 **Figure 4. Taxonomic profiling results for HM-277D data sets. (a)** Gene identification
368 performance of 20 bacterial strains. 3 gene sets (RefSeq, 16S rRNA, protein coding) were
369 evaluated. Colors indicate different metrics (exonic coverage and detection rate). Exonic
370 coverage (orange) is the percentage of exonic region covered by at least 1 read out of all
371 exons. Detection rate (blue) is the percentage of genes with coverage depth > 1 and
372 exonic coverage > 50% out of all genes. Gold standard abundance of each strain was
373 indicated in black. **(b)** Bacteria abundance estimation. Scatter plots abundance estimates
374 versus gold standard abundances from HM-277D mock community across taxonomic
375 ranks. Abundances were converted to log scale to facilitate viewing. Pearson correlation
376 and L1 norm were utilized to quantify the performance. Estimates consistently share a

377 good agreement with gold standard across ranks with correlation > 0.85 and L1 norm <
378 0.32. Abbreviations for bacterial name above the species level are listed below. Phylum
379 level: Actinobacteria, Bacteroidetes (Bac), Deinococcus-Thermus (Dei), Firmicutes (Fir),
380 Proteobacteria (Pro); Class level: Actinobacteria (Act), Alphaproteobacteria (Alp), Bacilli
381 (Bac), Bacteroidia (Bact), Betaproteobacteria (Bet), Clostridiales (Clo), Deinococcus
382 (Dei), Epsilonproteobacteria (Eps), Gammaproteobacteria (Gam); Order level:
383 Actinomycetales (Act), Bacillales (Bac), Bacteroidales (Bact), Campylobacterales (Cam),
384 Clostridiales (Clo), Deinococcales (Dei), Enterobacteriales (Ent), Lactobacillales (Lac),
385 Neisseriaceae (Nei), Propionibacteriaceae (Pro), Pseudomonadales (Pse),
386 Rhodobacterales (Rho); Family level: Actinomycetaceae (Act), Bacillaceae (Bac),
387 Bacteroidaceae (Bact), Clostridiaceae (Clo), Deinococcaceae (Dei), Enterobacteriaceae
388 (Ent), Enterococcaceae (Ent), Helicobacteraceae (Hel), Lactobacillaceae (Lac),
389 Listeriaceae (Lis), Moraxellaceae (Mor), Neisseriaceae (Nei), Propionibacteriaceae (Pro),
390 Pseudomonadaceae (Pse), Rhodobacteraceae (Rho), Staphylococcaceae (Sta); Genus
391 level: Acinetobacter (Act), Actinomyces (Act), Bacillus (Bac), Bacteroides (Bact),
392 Clostridium (Clo), Deinococcus (Dei), Enterococcus (Ent), Escherichia (Esc),
393 Helicobacter (Hel), Lactobacillus (Lac), Listeria (Lis), Neisseria (Nei), Propionibacterium
394 (Pro), Pseudomonas (Pse), Rhodobacter (Rho), Staphylococcus (Sta), Streptococcus
395 (Str).

396

397 **Discussion**

398 Complete genome assembly and population profiling are critical for the interpretation of
399 microbial community diversity. However, a benchmarking long-read data set with
400 consistent evaluation metrics is still lacking, which has hindered our understanding of
401 long-read sequence data in metagenome assembly. In this study, we deeply sequenced
402 HM-276D and HM-277D samples to assess the performance of error-prone Nanopore

403 sequencing data and bioinformatics tools in characterizing microbial community.
404 Assemblers consistently achieved high accuracy and completeness for nontrivial bacteria
405 strains and genome binners performed well at above the genus level. Furthermore, by
406 targeting on marker genes, we were able to identify rare strains with extremely low
407 abundance in microbial community. Overall, our results have demonstrated that the
408 technical feasibility to characterize complete microbial genomes and populations from
409 Nanopore sequencing data with metagenomic software.

410 We note that despite the feasibility to characterize complete microbial genomes from
411 long-read sequencing data, there are still challenges to be resolved in our study. Even for
412 evenly mixed samples, the best performing assembler meta-flye achieve 99.99%
413 consensus accuracy. However, as the reference genomes contains 70 Mb, 0.04% error
414 rate has led to 28 Kbp of mismatches. These erroneous bases could be due to
415 sequencing errors in low quality read, a major drawback of long-read sequence data and
416 base modification, which may complicate the genome assembly. To prevent these errors,
417 a sequencer with unbiased and methylation-aware base caller is in need. (We also
418 acknowledge that some of the mismatches may be due to natural differences between
419 reference microbiome samples and the reference genomes that were used.) In addition,
420 there is still room for further improvement in assembly completeness by using longer
421 reads or better designed assemblers to account for long repeats in genomes. In our study,
422 we assembled long-read sequenced data from 20 bacterial strains across species.
423 However, the performance at strain-level still remains unknown as closely related
424 genomes is always a major challenge for genome assembly. In the future, we anticipate

425 that more mock microbial community will be released with bacteria at strain level for
426 benchmarking study.

427 By evaluating the performance of bioinformatics tools across different technologies, we
428 found that third generation sequencing generally facilitates the complete characterization
429 of complex bacterial genomes by overcoming many limitations of second generation
430 sequencing. The short read length has limited the ability of Illumina sequencing in
431 genome interpretation. For example, the length of repetitive genomic region is larger than
432 a single read. As a consequence, intra- and intergenomic diversities are unlikely to be
433 captured by short sequencing data. This issue has been resolved by long-read
434 sequencing technologies (ONT and PacBio), which is able to span low complexity and
435 repetitive regions by providing sequence reads with at least 10 kb in length. While
436 generating data with much higher error rate than PacBio, ONT has become a promising
437 platform in many applications, especially for studies requiring large amounts of data. This
438 is because ONT provides longer reads (up to 900 kb in length) with higher throughput
439 compared to PacBio (10-15 kb in length). Moreover, ONT is currently more affordable
440 with lower per-base cost of data generation, which is a key factor in long-read sequencing
441 studies. Overall, the application of these two major long-read sequencing platforms in
442 metagenomics analysis of complex communities is still restricted by higher error rate. This
443 problem could be addressed with improvement of consensus sequences. Recently, newly
444 released R10 chip from ONT has longer base-contacting constriction in the pore, which
445 improves the homopolymer resolution as compared to R9. This can lead to metagenome
446 assembly with higher accuracy and completeness, as well as more accurate OTU
447 identification. Future metagenomics studies are expected to be changed dramatically by

448 this approach. For example, strain UA159 and NN2025 under species *Streptococcus*
449 *mutans* only share 8% common regions, which can be uniquely assigned. We then found
450 that 20% of ONT reads can cover the unique region of these two strains respectively,
451 which is infeasible for short reads. Therefore, with better quality of long-read data, this
452 approach may allow us to identify bacteria of interest directly at strain level instead of
453 performing binning analysis in the future.

454 In addition to illustrating the advantages brought by long-read sequence data, we also
455 assessed the performance of four *de novo* assembly algorithms and a long-read genome
456 binner. The bioinformatics challenges to interpret rich information from complex microbial
457 community include high error rates and low throughput for long-read sequencing,
458 fragmented nature for short-read sequencing, and large CPU hours requirement. For
459 evenly mixed (each with 5% abundance) HM-276D mock community, 4 tools consistently
460 achieved high accuracy and completeness. No single assembler significantly outperforms
461 others. By subsampling data to less coverage depths, not surprisingly, we found that the
462 corresponding metrics for 4 tools decreased. In terms of speed, wtdbg2 is tens of times
463 faster than other tools. For the unevenly mixed mock community HM-277D, assembly
464 accuracy still remain high for all 4 tools (~97-98%). Genome fraction was reduced
465 because 13 rare bacterial strains (<1%) were poorly assembled. Hybrid-assembler
466 OPERA-MS, which combines the advantages from long and short-read technologies,
467 shows more robust performance to bacterial strains with extremely low abundance than
468 other tools. However, it produced much more contigs with less contiguity while meta-flye,

469 Canu and wtdbg2 returned single contig for 18, 15 and 17 strains respectively.
470 Furthermore, taxonomic binning results show that Megan-LR performs well when
471 genomes are not closely related. Taxon bins were reconstructed with acceptable
472 accuracy down to the genus level while performance decreased at species and strain
473 level.

474 In summary, our results demonstrate the feasibility to characterize complete microbial
475 genomes and populations from error-prone Nanopore sequencing data, but also highlight
476 necessary bioinformatics improvements for future metagenomics tool development to
477 handle specific challenges in error-prone long-read sequencing data. We believe that
478 future metagenomics studies will benefit from this approach to assemble complete
479 microbial genomes, while maintaining the theoretical ability to detect DNA methylations
480 and base modifications, infer repetitive elements and structural variants, and achieve
481 strain-level resolution within microbial communities. All the data sets on reference
482 microbiomes are made publicly available to facilitate benchmarking studies on
483 metagenomics and the development of novel software tools.

484 **Methods and materials**

485 **Oxford nanopore sequencing of HM-276D and HM-277D**

486 DNA samples of HM-276D and HM-277D were ordered from BEI Resources.
487 Concentration of DNA was assessed using the dsDNA HS assay on a Qubit fluorometer
488 (Thermo Fisher).

489 For library preparation, 1.0 µg DNA was used as the input DNA of each library. The library
490 was prepared using the ligation sequencing protocol (SQK-LSK109) from ONT.
491 Concretely, end repair, dA-tailing and DNA repair was performed using NEBNext Ultra II
492 End Repair/dA-tailing Module (catalog No. E7546) and NEBNext FFPE Repair Mix
493 (M6630). In all, 3.5 µl Ultra II End-prep reaction buffer, 3 µl Ultra II End-prep enzyme mix,
494 3.5 µl NEBNext FFPE DNA Repair Buffer and 2 µl NEBNext FFPE DNA Repair Mix were
495 added to the input DNA. The total volume was adjusted to 60 µl by adding nuclease-free
496 water (NFW). The mixture was incubated at 20 °C for 5 min and 65 °C for 5 min. A
497 1 × volume (60 µl) AMPure XP clean-up was performed and the DNA was eluted in 61 µl
498 NFW. One microliter of the eluted dA-tailed DNA was quantified using the Qubit
499 fluorometer. A total of 0.7 µg DNA should be retained if the process is successful.

500 Adaptor ligation was performed using the following steps. Five microliter Adaptor Mix
501 (ONT, SQK-LSK109 Kit), 25 µl Ligation Buffer (ONT, SQK-LSK109 Kit) and 10 µl
502 NEBNext Quick T4 DNA Ligase (NEB, catalog No. E6056) were added to the 60 µl dA-
503 tailed DNA from the previous step. The mixture was incubated at room temperature for
504 10 min. The adaptor-ligated DNA was cleaned up using 40 µl AMPure XP beads. The
505 mixture of DNA and AMPure XP beads was incubated for 5 min at room temperature and
506 the pellet was washed twice by 250 µl Long Fragment Buffer (ONT, SQK-LSK109). The
507 purified-ligated DNA was resuspended in 15 µl Elution Buffer (ONT, SQK-LSK109). A 1-
508 µl aliquot was quantified by fluorometry (Qubit) to ensure ≥ 400 ng DNA was retained.
509 The final library was prepared by mixing 37.5 µl Sequencing Buffer (ONT, SQK-LSK109),
510 25.5 µl Loading Beads (ONT, SQK-LSK109), and 12 µl purified-ligated DNA. The library
511 was loaded to R9.4 flow cells (FLO-MIN106, ONT) according to the manufacturer's

512 guidelines. GridION sequencing was performed using default settings for the R9.4 flow
513 cell and SQK-LSK109 library preparation kit. The sequencing was controlled and
514 monitored using the MinKNOW software developed by ONT.

515

516 **Metagenome assembly**

517 Genome assemblies of the 20-mixed bacteria from HM-276D and MH-277D mock
518 communities were conducted using 4 existing assemblers based on generated long-read
519 sequencing reads. These 4 dedicated long-read assemblers we used are wtdbg2 (v2.4),
520 OPERA-MS, Canu (v1.8) and meta-flye, where Canu and meta-flye are designed to be
521 capable to handle metagenome while wtdbg2 and OPERA-MS are for broadly application.
522 To evaluate the impact of coverage depth in genome assembly, in addition to 525x (HM-
523 276D) and 1068x (HM-277D), we subsampled 5 data sets with 365x, 160x, 80x, 40x and
524 20x coverages for these two mock communities. In addition to long-read data, OPERA-
525 MS requires short reads to improve the assembly accuracy. Hence, we downloaded
526 Illumina sequenced HM-276D[5] and HM-277D data sets[38]. Similarly, these short-read
527 data were also subsampled with depths 160x, 80x, 40x and 20x, which were provided to
528 OPERA-MS in corresponding data set analysis. We also analyzed a PacBio data set[33]
529 of HM-276D sample using wtdbg2, OPERA-MS, Canu and meta-flye to compare
530 assembly performance across sequencing technologies. For comparison fairness, we
531 applied consistent configuration settings for each tool across different coverage depths.
532 In specific, we specified estimated genome size as 70M, where the parameters are “-x
533 ont -g 70m -t 20” for wtdbg2, “genomeSize=70M useGrid=True” for Canu, and

534 “CONTIG_LEN_THR 500, CONTIG_EDGE_LEN 80, CONTIG_WINDOW_LEN 340,
535 KMER_SIZE 60, LONG_READ_MAPPER minimap2” for OPERA-MS, “-t 40 -g 70m -o ./
536 --meta” for meta-flye. 40 contig output files were obtained (2 mock community samples,
537 6 depths of coverage, 4 assembly tools) for further evaluation.

538

539 **Metagenome assembly evaluation**

540 Assembled genomes produced by each tool based on different samples and coverage
541 depths were evaluated with metrics related to contiguity, genome completeness and
542 accuracy. To assess the assembly contiguity, we first used our script to calculate the
543 widely-used statistic N50, which is the shortest contig needed to cover at least 50% of the
544 assembly. In addition, other related statistics, such as number of contigs, number of long
545 contigs (>10kb), longest contigs and total assembly size, were collected from the FASTA
546 output file of each assembler. Furthermore, we summarized NG50 for each method by
547 replacing the assembly size with estimated genome size. This quantity represents the
548 shortest contig needed to cover 50% of the genome. Based on these metrics, the
549 contiguity of assemblies was comprehensively evaluated. Next, we downloaded the
550 reference genome FASTA files of all 20 bacteria from NCBI database to measure the
551 concordance between the references and assemblies. First, assemblies were mapped to
552 the reference genomes using Mummer v3.23 with parameters “-maxmatch -c 100 -p
553 nucmer”. Then, by comparing all contigs mapped onto the reference using dandiff,
554 assembly accuracy was calculated using 1-to-1 alignment identity, which is the correctly
555 matched base-pair percentage of contigs uniquely mapped to the reference genome (1-

556 mismatch%). In addition, to assess the assembly completeness, we calculated the
557 percentage of genome covered by the contigs. In real case, instead of evenly mixed in
558 HM-276D mock community, bacterial strains are non-uniformly distributed, where some
559 are likely to share extremely low abundance. Therefore, we evaluated the impact of the
560 genomic DNA abundance on genome assembly. For the unevenly mixed HM-277D mock
561 community samples, we calculated the abundance for each bacterial strain by normalizing
562 the concentration with related reference genome size. The relationship between
563 abundances and assessment metrics was displayed using scatter plots. For each plot,
564 linearity was measured based on Spearman correlation using R v3.3.3.

565

566 **Taxonomic binning analysis**

567 Taxon bins of the 20-mixed bacteria from two mock communities were recovered using
568 taxonomic binner Megan-LR[25] with 3 long-read sequencing data sets: HM-276D
569 (Nanopore, PacBio) and HM-277D (Nanopore) at 160x depth of coverage. We first
570 aligned all reads against NCBI-nr protein reference database using LAST with parameters
571 “-P 100 -F15”. Next, output MAF files were converted to DAA format in smaller size. Then,
572 we meganized the DAA files using MEGAN[26], which allows us to interactively visualize
573 and explore these taxonomic results. To evaluate the taxonomic binning performance, we
574 first counted the number of reads and bases which were correctly assigned to each taxon
575 from the mock microbial community. We determined the metrics (precision, sensitivity,
576 true positive rate and false positive rate). Precision and sensitivity assess how accuracy
577 each read is classified across different sequencing technologies. Precision is the

578 percentage of reads assigned correctly to the corresponding taxa out of all reads.
579 Sensitivity is the percentage of correct reads out of reads assigned to the particular taxa.
580 Next, we use true positive rate (TPR) and false discover rate (FDR) to assess the
581 accuracy in taxonomic detection across sequencing technologies. TPR is the percentage
582 of correctly detected taxon out of known taxon from the microbial community. FDR is the
583 percentage of correctly detected taxon out of all detected taxon. All metrics are defined
584 at each taxonomic rank.

585 **Acknowledgements**

586 This work was supported by CHOP Research Institute to K.W..

587 The following reagent was obtained through BEI Resources, NIAID, NIH as part of the
588 Human Microbiome Project: Genomic DNA from Microbial Mock Community B
589 (Staggered, High Concentration), v5.2H, for Whole Genome Shotgun Sequencing, HM-
590 277D.

591 The following reagent was obtained through BEI Resources, NIAID, NIH as part of the
592 Human Microbiome Project: Genomic DNA from Microbial Mock Community B (Even,
593 High Concentration), v5.1H, for Whole Genome Shotgun Sequencing, HM-276D.

594 **Competing interests**

595 The authors declare no conflict of interest.

596

597 References

- 598 1. Gill SR, Pop M, Deboy RT, Eckburg PB, Turnbaugh PJ, Samuel BS, Gordon JI, Relman DA, Fraser-
599 Liggett CM, Nelson KE: **Metagenomic analysis of the human distal gut microbiome.** *Science* 2006,
600 **312**:1355-1359.
- 601 2. Lewis JD, Chen EZ, Baldassano RN, Otley AR, Griffiths AM, Lee D, Bittinger K, Bailey A, Friedman
602 ES, Hoffmann C, et al: **Inflammation, Antibiotics, and Diet as Environmental Stressors of the Gut**
603 **Microbiome in Pediatric Crohn's Disease.** *Cell Host Microbe* 2015, **18**:489-500.
- 604 3. Chehoud C, Albenberg LG, Judge C, Hoffmann C, Grunberg S, Bittinger K, Baldassano RN, Lewis JD,
605 Bushman FD, Wu GD: **Fungal Signature in the Gut Microbiota of Pediatric Patients With**
606 **Inflammatory Bowel Disease.** *Inflamm Bowel Dis* 2015, **21**:1948-1956.
- 607 4. Hooper LV, Stappenbeck TS, Hong CV, Gordon JI: **Angiogenins: a new class of microbicidal**
608 **proteins involved in innate immunity.** *Nat Immunol* 2003, **4**:269-273.
- 609 5. Jones MB, Highlander SK, Anderson EL, Li W, Dayrit M, Klitgord N, Fabani MM, Seguritan V, Green
610 J, Pride DT, et al: **Library preparation methodology can influence genomic and functional**
611 **predictions in human microbiome research.** *Proc Natl Acad Sci U S A* 2015, **112**:14024-14029.
- 612 6. Ley RE, Turnbaugh PJ, Klein S, Gordon JI: **Microbial ecology: human gut microbes associated with**
613 **obesity.** *Nature* 2006, **444**:1022-1023.
- 614 7. Liang X, Bittinger K, Li X, Abernethy DR, Bushman FD, FitzGerald GA: **Bidirectional interactions**
615 **between indomethacin and the murine intestinal microbiota.** *Elife* 2015, **4**:e08973.
- 616 8. Sartor RB: **Microbial influences in inflammatory bowel diseases.** *Gastroenterology* 2008,
617 **134**:577-594.
- 618 9. Schaubert J, Svanholm C, Termen S, Iffland K, Menzel T, Scheppach W, Melcher R, Agerberth B,
619 Luhrs H, Gudmundsson GH: **Expression of the cathelicidin LL-37 is modulated by short chain fatty**
620 **acids in colonocytes: relevance of signalling pathways.** *Gut* 2003, **52**:735-741.
- 621 10. Turnbaugh PJ, Hamady M, Yatsunenko T, Cantarel BL, Duncan A, Ley RE, Sogin ML, Jones WJ, Roe
622 BA, Affourtit JP, et al: **A core gut microbiome in obese and lean twins.** *Nature* 2009, **457**:480-484.
- 623 11. Wang F, Kaplan JL, Gold BD, Bhasin MK, Ward NL, Kellermayer R, Kirschner BS, Heyman MB, Dowd
624 SE, Cox SB, et al: **Detecting Microbial Dysbiosis Associated with Pediatric Crohn Disease Despite**
625 **the High Variability of the Gut Microbiota.** *Cell Rep* 2016, **14**:945-955.
- 626 12. Wen L, Ley RE, Volchkov PY, Stranges PB, Avanesyan L, Stonebraker AC, Hu C, Wong FS, Szot GL,
627 Bluestone JA, et al: **Innate immunity and intestinal microbiota in the development of Type 1**
628 **diabetes.** *Nature* 2008, **455**:1109-1113.

- 629 13. Wu GD, Chen J, Hoffmann C, Bittinger K, Chen YY, Keilbaugh SA, Bewtra M, Knights D, Walters WA,
630 Knight R, et al: **Linking long-term dietary patterns with gut microbial enterotypes.** *Science* 2011,
631 **334**:105-108.
- 632 14. Group NHW, Peterson J, Garges S, Giovanni M, McInnes P, Wang L, Schloss JA, Bonazzi V, McEwen
633 JE, Wetterstrand KA, et al: **The NIH Human Microbiome Project.** *Genome Res* 2009, **19**:2317-
634 2323.
- 635 15. Janda JM, Abbott SL: **16S rRNA gene sequencing for bacterial identification in the diagnostic
636 laboratory: pluses, perils, and pitfalls.** *J Clin Microbiol* 2007, **45**:2761-2764.
- 637 16. Quince C, Walker AW, Simpson JT, Loman NJ, Segata N: **Shotgun metagenomics, from sampling
638 to analysis.** *Nat Biotechnol* 2017, **35**:833-844.
- 639 17. Hao X, Chen T: **OTU analysis using metagenomic shotgun sequencing data.** *PLoS One* 2012,
640 **7**:e49785.
- 641 18. Chen EZ, Bushman FD, Li H: **A Model-Based Approach For Species Abundance Quantification
642 Based On Shotgun Metagenomic Data.** *Stat Biosci* 2017, **9**:13-27.
- 643 19. Ruan J, Li H: **Fast and accurate long-read assembly with wtdbg2.** *Nat Methods* 2019.
- 644 20. Bertrand D, Shaw J, Kalathiyappan M, Ng AHQ, Kumar MS, Li C, Dvornicic M, Soldo JP, Koh JY, Tong
645 C, et al: **Hybrid metagenomic assembly enables high-resolution analysis of resistance
646 determinants and mobile elements in human microbiomes.** *Nat Biotechnol* 2019, **37**:937-944.
- 647 21. Koren S, Walenz BP, Berlin K, Miller JR, Bergman NH, Phillippy AM: **Canu: scalable and accurate
648 long-read assembly via adaptive k-mer weighting and repeat separation.** *Genome Res* 2017,
649 **27**:722-736.
- 650 22. Kolmogorov M, Yuan J, Lin Y, Pevzner PA: **Assembly of long, error-prone reads using repeat
651 graphs.** *Nat Biotechnol* 2019, **37**:540-546.
- 652 23. Li D, Liu CM, Luo R, Sadakane K, Lam TW: **MEGAHIT: an ultra-fast single-node solution for large
653 and complex metagenomics assembly via succinct de Bruijn graph.** *Bioinformatics* 2015,
654 **31**:1674-1676.
- 655 24. Gregor I, Droge J, Schirmer M, Quince C, McHardy AC: **PhyloPythiaS+: a self-training method for
656 the rapid reconstruction of low-ranking taxonomic bins from metagenomes.** *PeerJ* 2016,
657 **4**:e1603.
- 658 25. Huson DH, Albrecht B, Bagci C, Bessarab I, Gorska A, Jolic D, Williams RBH: **MEGAN-LR: new
659 algorithms allow accurate binning and easy interactive exploration of metagenomic long reads
660 and contigs.** *Biol Direct* 2018, **13**:6.

- 661 26. Huson DH, Beier S, Flade I, Gorska A, El-Hadidi M, Mitra S, Ruscheweyh HJ, Tappu R: **MEGAN**
662 **Community Edition - Interactive Exploration and Analysis of Large-Scale Microbiome**
663 **Sequencing Data.** *PLoS Comput Biol* 2016, **12**:e1004957.
- 664 27. Francis OE, Bendall M, Manimaran S, Hong C, Clement NL, Castro-Nallar E, Snell Q, Schaalje GB,
665 Clement MJ, Crandall KA, Johnson WE: **Pathoscope: species identification and strain attribution**
666 **with unassembled sequencing data.** *Genome Res* 2013, **23**:1721-1729.
- 667 28. Hong C, Manimaran S, Shen Y, Perez-Rogers JF, Byrd AL, Castro-Nallar E, Crandall KA, Johnson WE:
668 **PathoScope 2.0: a complete computational framework for strain identification in**
669 **environmental or clinical sequencing samples.** *Microbiome* 2014, **2**:33.
- 670 29. Byrd AL, Perez-Rogers JF, Manimaran S, Castro-Nallar E, Toma I, McCaffrey T, Siegel M, Benson G,
671 Crandall KA, Johnson WE: **Clinical PathoScope: rapid alignment and filtration for accurate**
672 **pathogen identification in clinical samples using unassembled sequencing data.** *BMC*
673 *Bioinformatics* 2014, **15**:262.
- 674 30. Jovel J, Patterson J, Wang W, Hotte N, O'Keefe S, Mitchel T, Perry T, Kao D, Mason AL, Madsen KL,
675 Wong GK: **Characterization of the Gut Microbiome Using 16S or Shotgun Metagenomics.** *Front*
676 *Microbiol* 2016, **7**:459.
- 677 31. Laudadio I, Fulci V, Palone F, Stronati L, Cucchiara S, Carissimi C: **Quantitative Assessment of**
678 **Shotgun Metagenomics and 16S rDNA Amplicon Sequencing in the Study of Human Gut**
679 **Microbiome.** *OMICS* 2018, **22**:248-254.
- 680 32. Ranjan R, Rani A, Metwally A, McGee HS, Perkins DL: **Analysis of the microbiome: Advantages of**
681 **whole genome shotgun versus 16S amplicon sequencing.** *Biochem Biophys Res Commun* 2016,
682 **469**:967-977.
- 683 33. Lee CH, Bowman B, Hall R: **Developments in PacBio® metagenome sequencing: Shotgun whole**
684 **genomes and full-length 16S.** In *International Plant and Animal Genome Conference Asia*. 2014
- 685 34. Sczyrba A, Hofmann P, Belmann P, Koslicki D, Janssen S, Droge J, Gregor I, Majda S, Fiedler J,
686 Dahms E, et al: **Critical Assessment of Metagenome Interpretation-a benchmark of**
687 **metagenomics software.** *Nat Methods* 2017, **14**:1063-1071.
- 688 35. Mason CE, Afshinnkoo E, Tighe S, Wu S, Levy S: **International Standards for Genomes,**
689 **Transcriptomes, and Metagenomes.** *J Biomol Tech* 2017, **28**:8-18.
- 690 36. Nicholls SM, Quick JC, Tang S, Loman NJ: **Ultra-deep, long-read nanopore sequencing of mock**
691 **microbial community standards.** *Gigascience* 2019, **8**.
- 692 37. McIntyre ABR, Alexander N, Grigorev K, Bezdan D, Sichtig H, Chiu CY, Mason CE: **Single-molecule**
693 **sequencing detection of N6-methyladenine in microbial reference materials.** *Nat Commun* 2019,
694 **10**:579.

695 38. Kuleshov V, Jiang C, Zhou W, Jahanbani F, Batzoglou S, Snyder M: **Synthetic long-read sequencing**
696 **reveals intraspecies diversity in the human microbiome.** *Nat Biotechnol* 2016, **34**:64-69.

697 39. Leggett RM, Alcon-Giner C, Heavens D, Caim S, Brook TC, Kujawska M, Martin S, Hoyles L, Clarke
698 P, Hall LJ: **Rapid profiling of the preterm infant gut microbiota using nanopore sequencing aids**
699 **pathogen diagnostics.** *bioRxiv* 2018:180406.

700 40. Leger A, Leonardi T: **pycoQC, interactive quality control for Oxford Nanopore Sequencing.** *The*
701 *Journal of Open Source Software* 2019, **4**:1236.

702

703

704

705

706

707

708

709

710

711

712

713

714

715 **Supplementary Material for Evaluation of single-molecule long-read whole-genome**
716 **shotgun sequencing on characterizing reference microbiomes**

717 Yu Hu*, Li Fang*, Christopher Nicholson, Kai Wang[§]

718 [§] Correspondence to: wangk@email.chop.edu

719 *** These authors contributed equally to this work**

720

721

722

723

724

725

726

727

728

729

730

731

732

733

734

735 **Supplementary Tables**

736

Tools	Depth	N50 length	Accuracy (%)	Coverage fraction (%)	NG50 length	# contigs	# long contigs	Longest contig	Genome size
Canu	20x	717267	98.5	96.8	616530	298	254	2612567	65503873
	40x	1987236	99.07	99.29	1975600	132	112	6286130	67676017
	80x	2886059	99.24	99.86	2731942	62	57	6316623	68735511
	160x	3901381	99.27	99.93	3901381	60	52	6299115	68879111
	365x	2983818	99.28	99.83	2983818	64	58	6292103	68964121
	480x	3911963	99.4	99.81	3911963	83	65	6359094	69425747
OPERA-MS	20x	1122204	99.83	99.71	1122204	5117	201	6324007	67168904
	40x	2657727	99.96	99.99	2657727	1695	81	5220208	67629371
	80x	2835709	99.96	99.99	2732545	1921	74	4636570	67632885
	160x	2933262	99.95	98.45	2792941	2347	65	6255842	66580943
	365x	2938016	99.91	99.98	2938016	4734	64	6255878	67858470
	480x	2938019	99.92	99.98	2938019	4732	63	6255756	67892051
wtdbg2	20x	519021	95.95	91.26	400703	443	363	3338270	61551400
	40x	2371130	97.94	98.4	2253156	175	124	6222827	66248572
	80x	3152360	98.73	98.34	2920496	122	80	6230107	66026593
	160x	2863759	98.7	98.08	2863759	91	69	6242719	66161138
	365x	2706888	98.66	97.33	2706888	90	73	6251621	65543654
	480x	2968720	98.73	95.94	2942294	61	53	8884115	64898035
meta-flye	20x	1653589	98.96	98.76	1547909	223	206	5630982	66808399
	40x	2725547	99.43	99.97	2653197	64	52	6274273	67627825
	80x	2930772	99.52	99.99	2930772	59	43	6251934	67630110
	160x	3888260	99.54	99.97	3180529	61	39	6252579	67595608
	365x	3181836	99.62	99.98	2934283	88	44	6245780	67727067
	480x	3181822	99.62	99.99	2934277	89	43	6245565	67700317

737 **Supplementary Table 1. Comprehensive assembly statistics on HM-276D using**
 738 **Canu, OPERA-MS, wtdbg2 and meta-flye.**

739

740

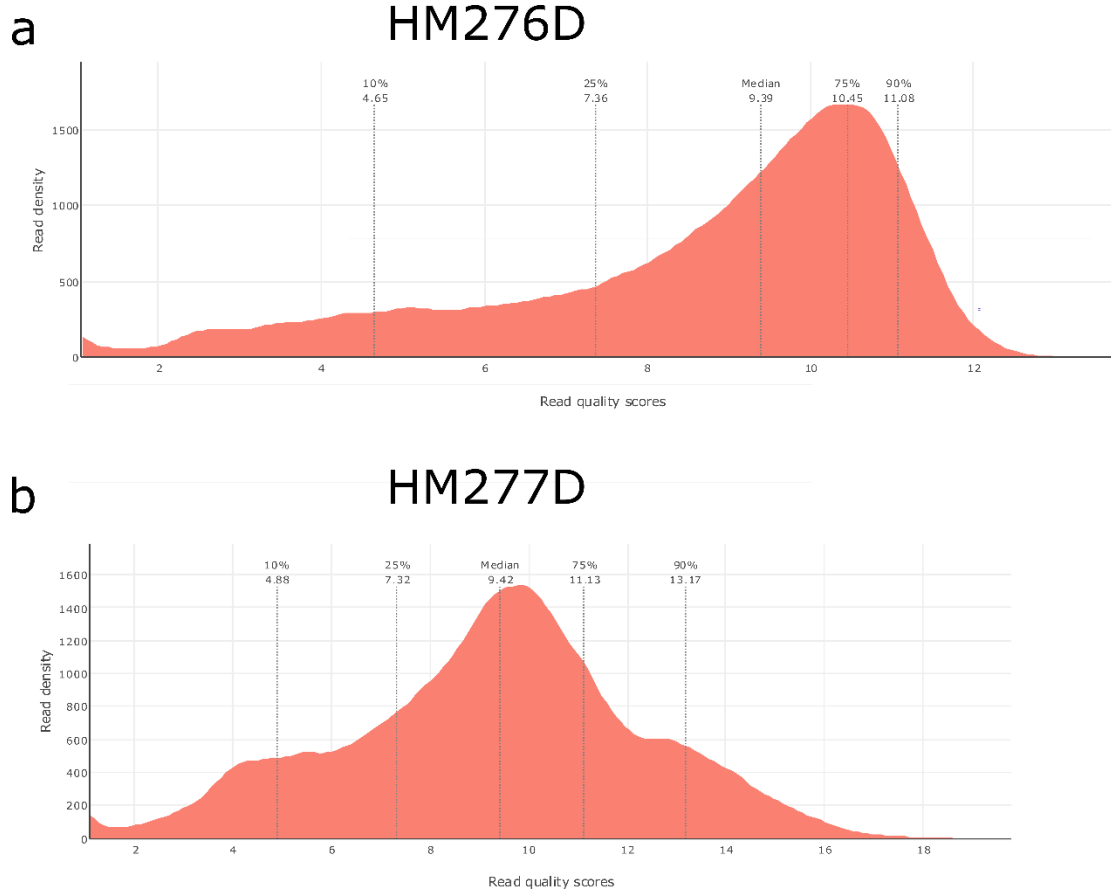
741

Species	Abundance	RefSeq gene		16S rRNA gene		Protein coding gene	
		average coverage (#bases)	Significantly detected gene	average coverage (#bases)	Significantly detected gene	average coverage (#bases)	Significantly detected gene
<i>Acinetobacter baumannii</i>	0.18%	9.83	94	9.50	6	9.86	3,817
<i>Actinomyces odontolyticus</i>	0.01%	4.27	56	3.10	2	4.65	1,999
<i>Bacillus cereus</i>	1.22%	100.51	138	94.04	12	102.33	5,675
<i>Bacteroides vulgatus</i>	0.02%	2.32	65	1.77	4	2.39	3,067
<i>Clostridium beijerinckii</i>	1.43%	96.40	143	78.49	14	97.42	5,149
<i>Deinococcus radiodurans</i>	0.03%	4.94	57	5.19	3	4.86	3,060
<i>Enterococcus faecalis</i>	0.01%	2.76	53	3.81	2	3.37	2,497
<i>Escherichia coli</i>	15.75%	1,032.93	179	1,003.79	7	1,060.46	4,341
<i>Helicobacter pylori</i>	0.07%	113.13	43	117.15	2	114.16	1,444
<i>Lactobacillus gasseri</i>	0.03%	27.95	96	24.06	6	28.97	1,783
<i>Listeria monocytogenes</i>	0.07%	10.74	184	8.92	6	11.42	2,864
<i>Neisseria meningitidis</i>	0.07%	42.67	71	28.53	4	47.85	1,926
<i>Propionibacterium acnes</i>	0.11%	41.60	58	38.75	3	43.02	2,506
<i>Pseudomonas aeruginosa</i>	5.01%	141.55	105	160.86	4	137.90	5,572
<i>Rhodobacter sphaeroides</i>	64.44%	2,219.40	67	1,993.22	3	2,438.52	4,279
<i>Staphylococcus aureus</i>	0.83%	323.26	79	289.00	5	404.68	2,982
<i>Staphylococcus epidermidis</i>	6.52%	976.37	76	1,117.10	5	1,002.43	2,472
<i>Streptococcus agalactiae</i>	0.03%	72.99	101	70.16	7	75.54	2,127
<i>Streptococcus mutans</i>	4.15%	4,207.60	80	3,598.02	5	3,818.93	1,953
<i>Streptococcus pneumoniae</i>	0.01%	1.91	58	1.30	2	2.39	1,868

742 **Supplementary Table 2. Species-specific gene coverage summary of HM-277D**
743 **data set.** Gene coverage statistics were summarized for 3 different gene sets: all
744 Refseq genes, 16S rRNA genes and protein coding genes. Average coverage = number
745 of bases mapped to the exonic region / length of exonic region. Gene is noted as
746 significantly detected when 50% exonic region is covered by at least 1 read and
747 average coverage > 1.

748

749 **Supplementary Figures**



750

751 **Supplementary Figure 1. Read quality of Nanopore sequencing data.** Read quality
752 of sequenced data sets, HM-276D **(a)** and HM-277D **(b)**, were summarized using
753 PycoQC respectively. Dashed lines indicate different quantiles (10%, 25%, 50%, 75%,
754 90%).

755

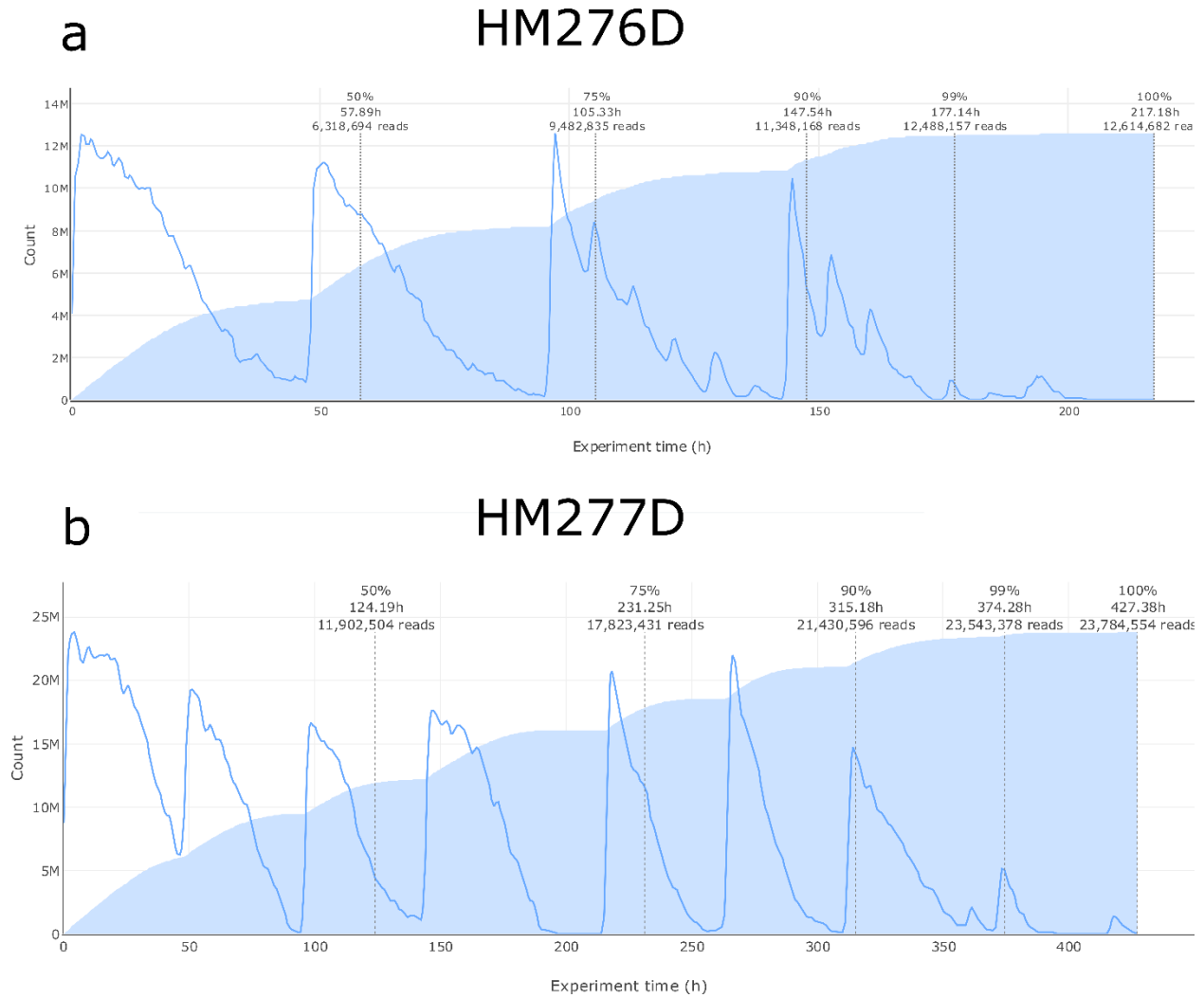
756

757

758

759

760



761

762 **Supplementary Figure 2. Read output over experiment of Nanopore sequencing**
763 **data.** Number of output reads over experiment time for sequenced data sets, HM-276D
764 **(a)** and HM-277D **(b)**, were summarized using PycoQC. Blue line indicates output velocity
765 at specific time. Shaded area represents cumulative read output over experiment time.

766

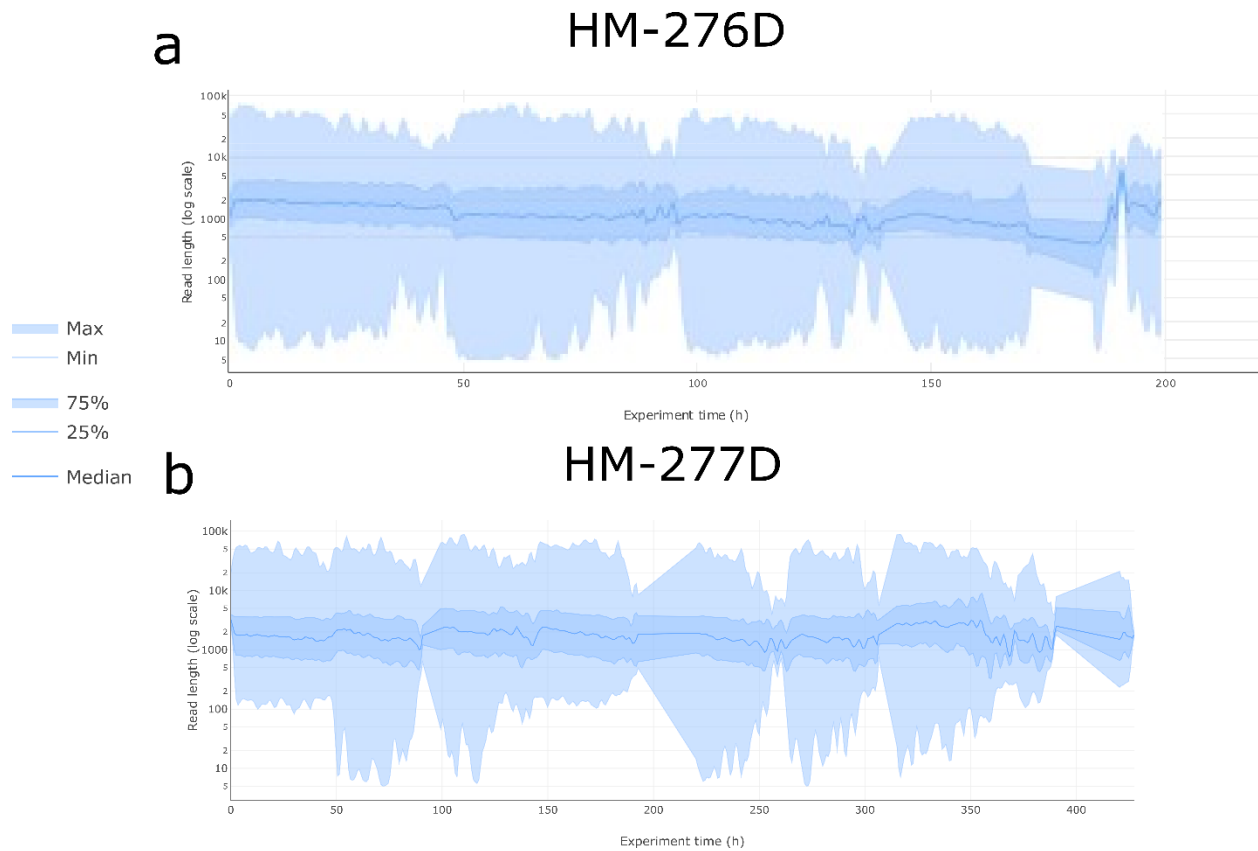
767

768

769

770

771



772

773 **Supplementary Figure 3. Read length over experiment of Nanopore sequencing**
774 **data.** Read length in log scale over experiment time for sequenced data sets, HM-276D
775 **(a)** and HM-277D **(b)**, were summarized using PycoQC.

776

777

778

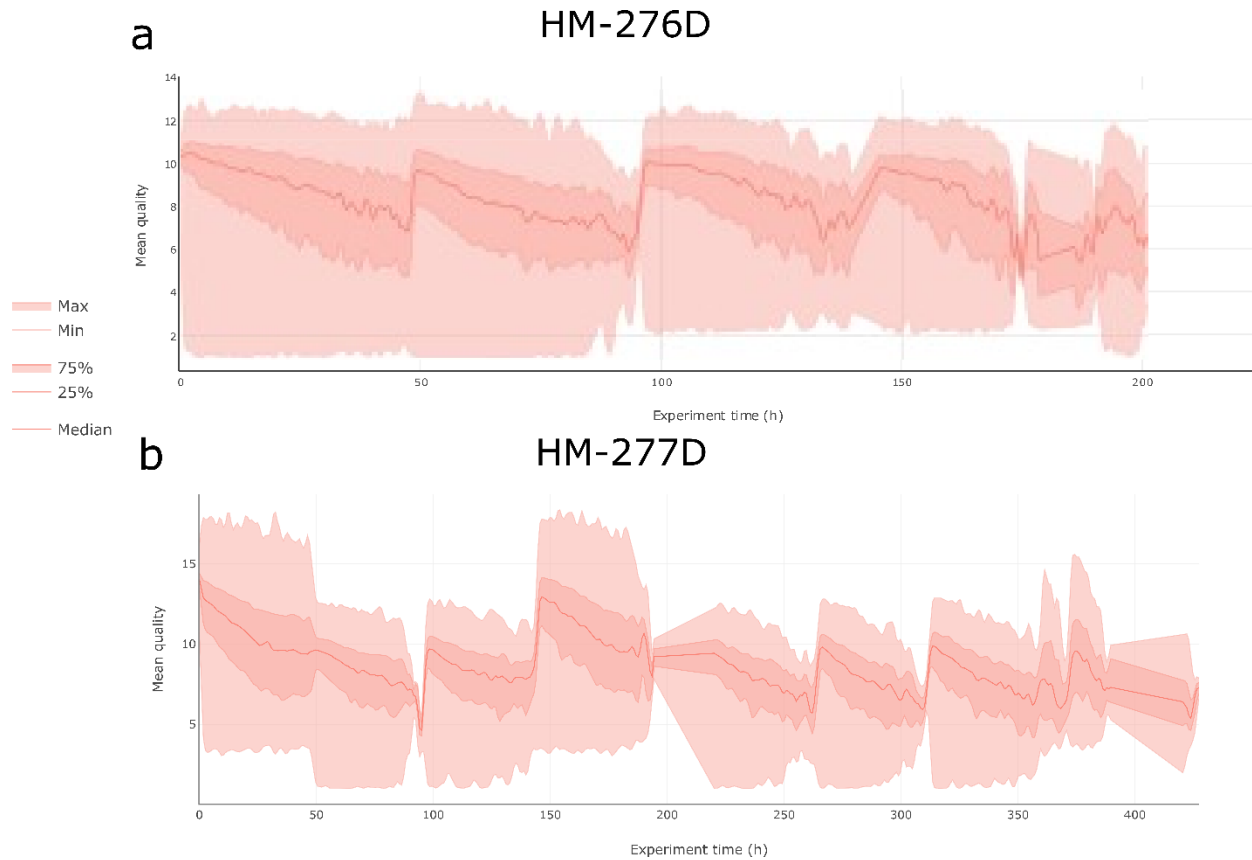
779

780

781

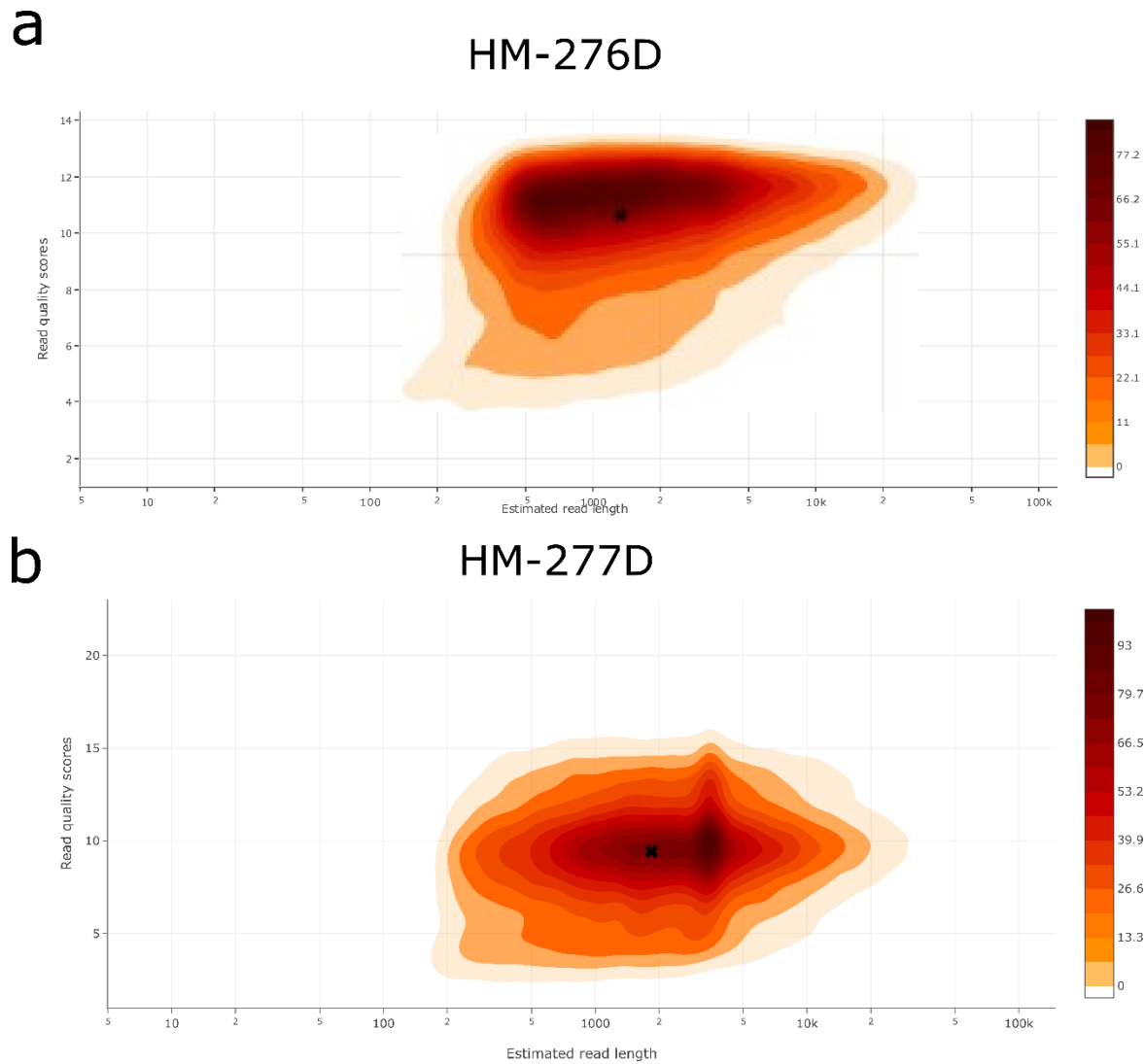
782

783



784

785 **Supplementary Figure 4. Read quality over experiment of Nanopore sequencing**
786 **data.** Mean read quality over experiment time for sequenced data sets, HM-276D **(a)**
787 and HM-277D **(b)**, were summarized using PycoQC.



788

789 **Supplementary Figure 5. Read quality score vs estimated read length.** Nanopore
790 read distribution of read length and quality score for sequenced data sets, HM-276D **(a)**
791 and HM-277D **(b)**, were summarized using PycoQC. Color indicates read density.

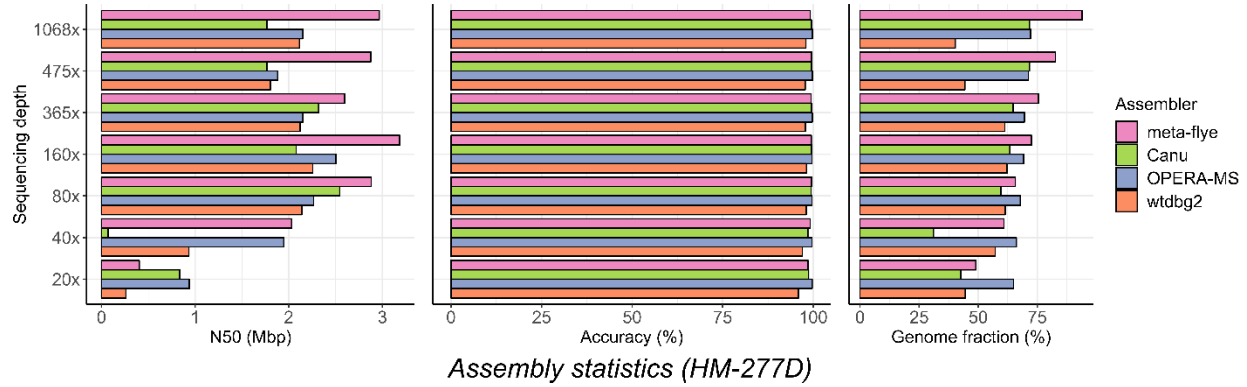
792

793

794

795

796



797

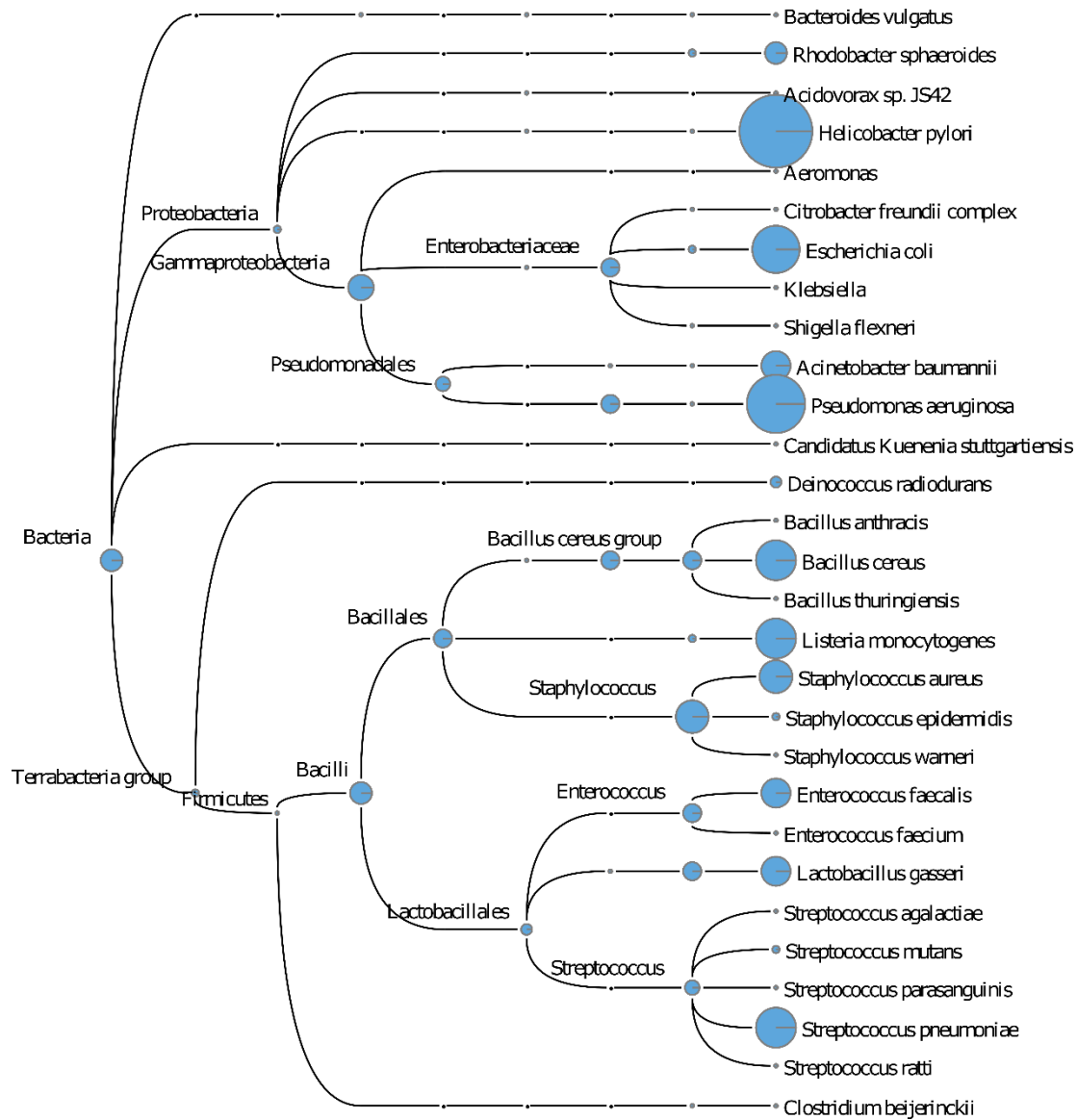
798 **Supplementary Figure 6. Assembly performance on HM-277D data set.** Assembly
799 statistics (N50 length, accuracy and genome fraction) of each assembler at different
800 coverage depths based on HM-277D data set. Colors indicate results from different
801 assemblers (Canu, OPERA-MS, wtdbg2, meta-flye). Assembly accuracy remains high
802 compared to HM-276D, ranging around ~99% across tools. N50 lengths and genome
803 fractions of all methods are substantially lower than even community.

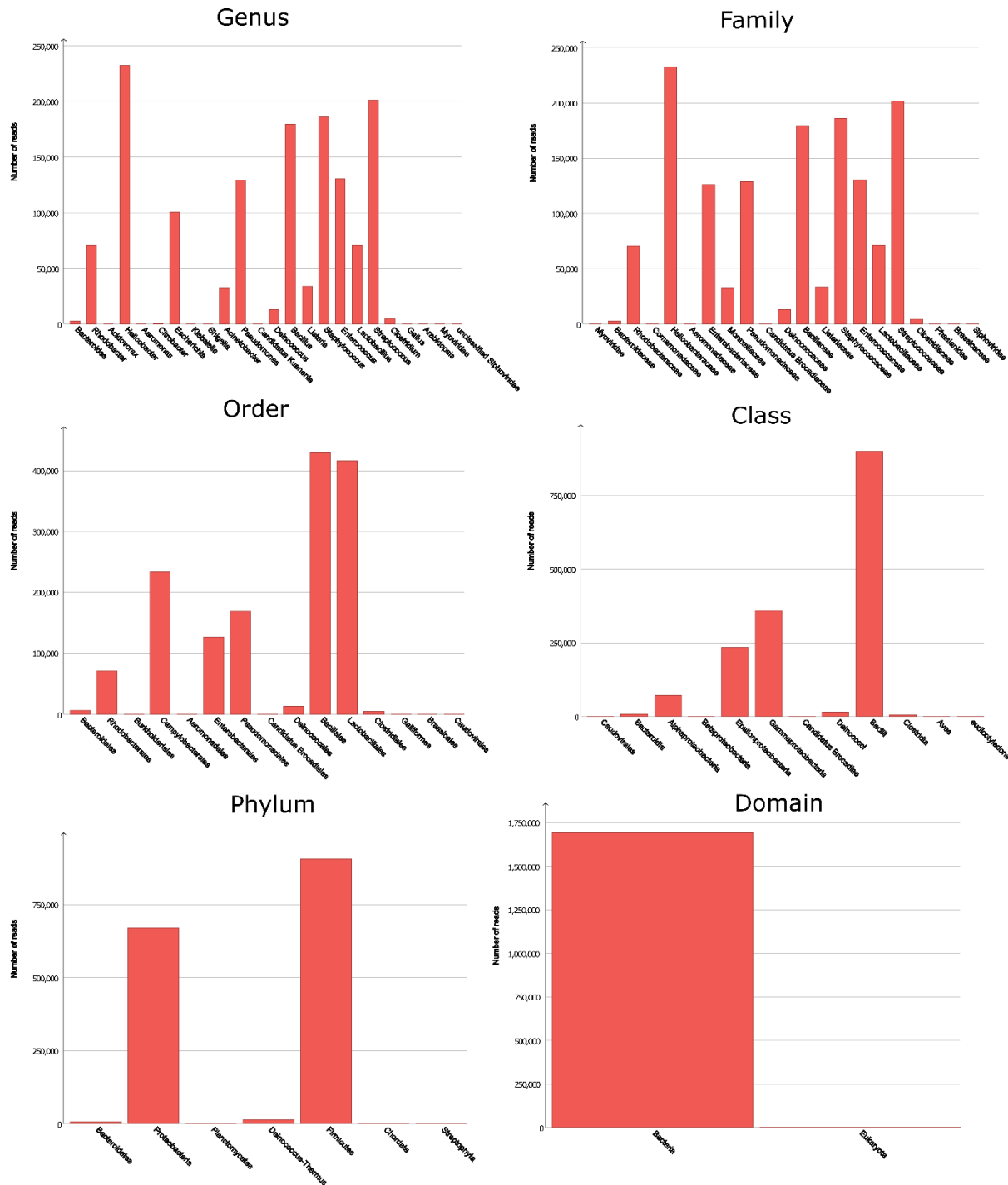
804

805

806

807

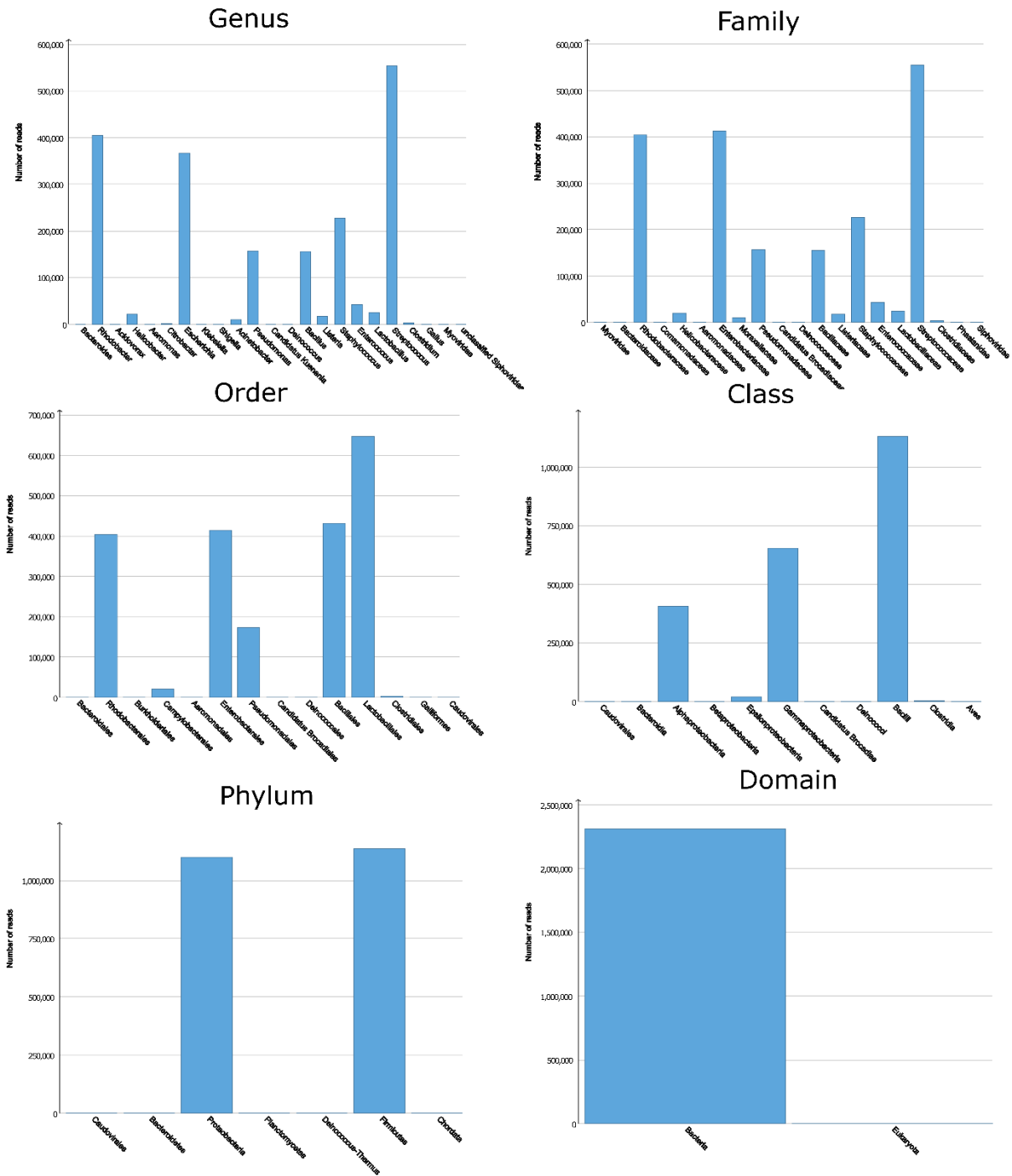




818

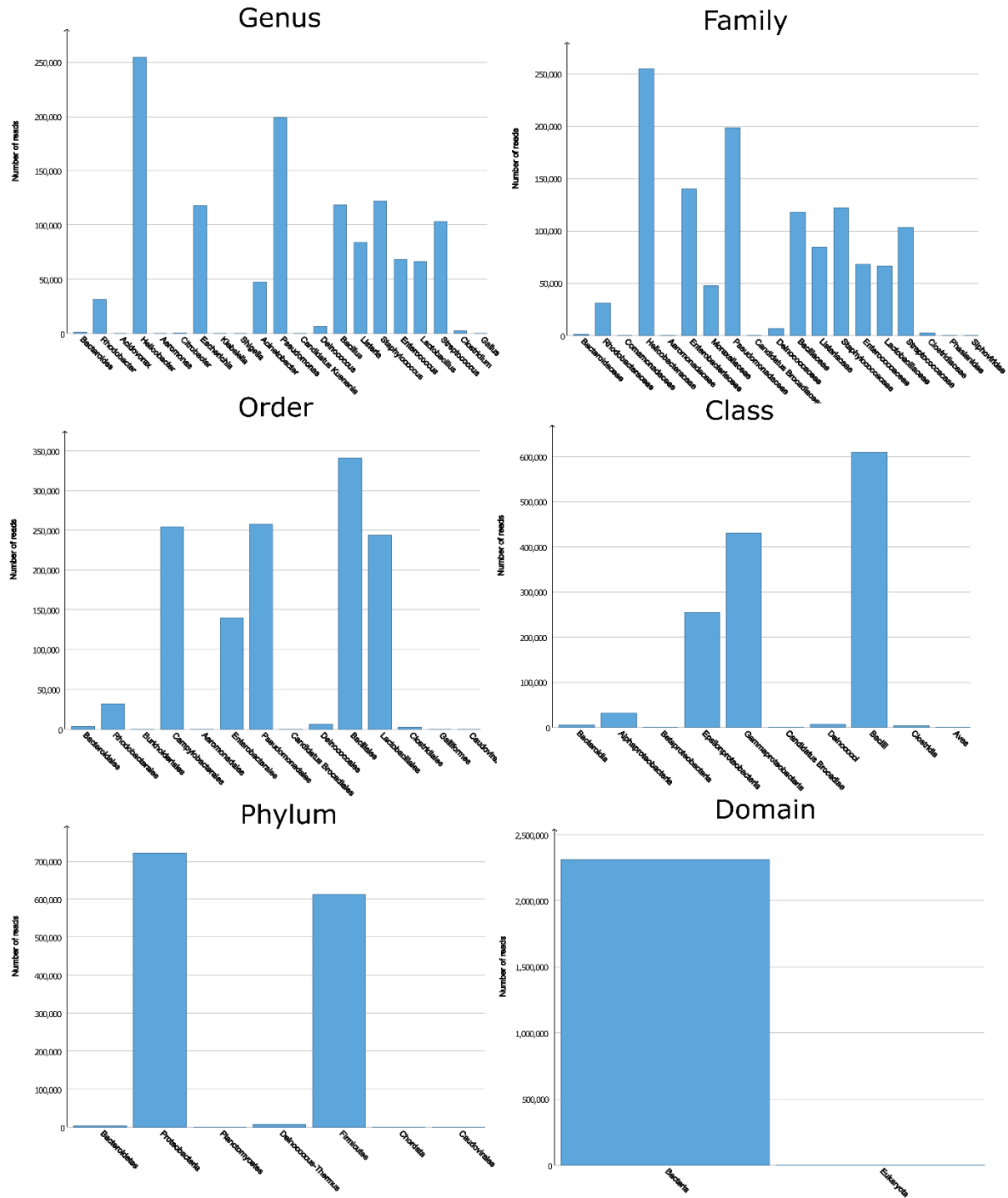
819 **Supplementary Figure 8. Megan taxonomic read distribution at different ranks**
 820 **obtained from HM-276 Nanopore sequenced data set.** HM-276D Nanopore data set
 821 was subsampled to 160x depth of coverage. Each read was aligned against NCBI-nr
 822 protein reference data base, then binned and visualized using Megan-LR.

823



824

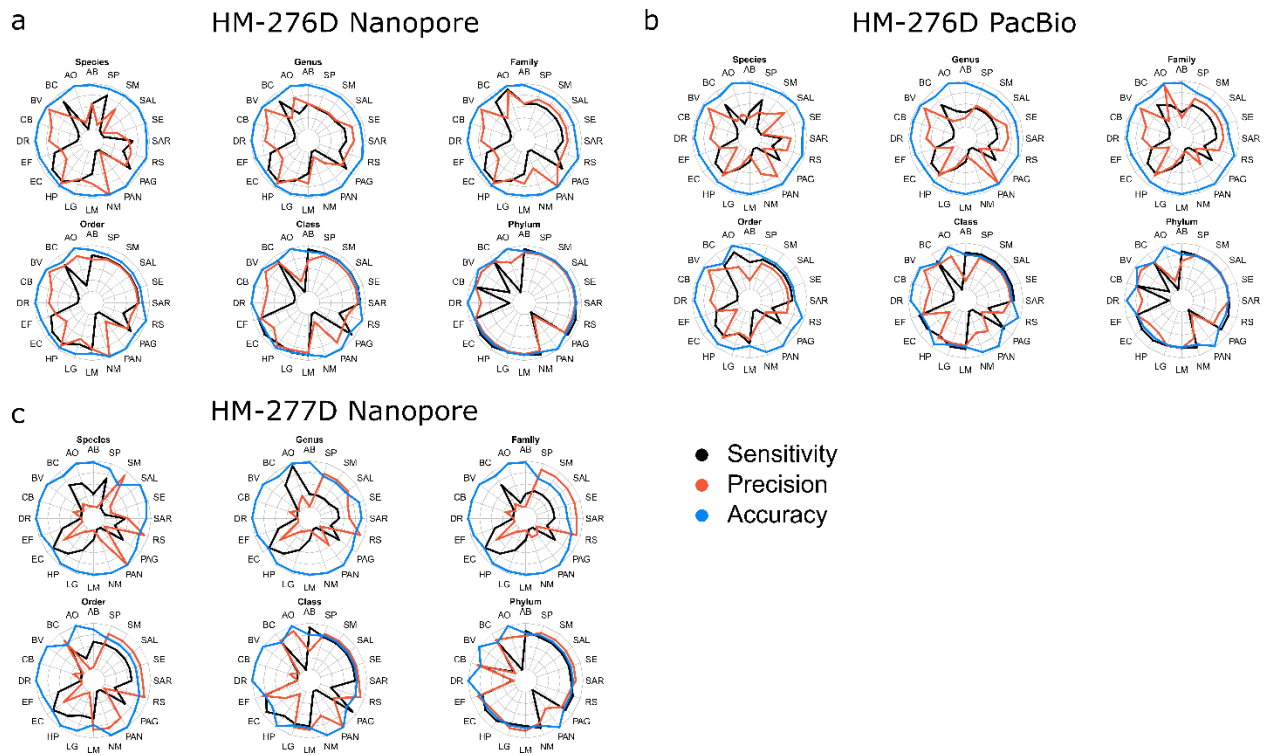
825 **Supplementary Figure 9. Megan taxonomic read distribution at different ranks**
 826 **obtained from HM-277 Nanopore sequenced data set.** HM-277D Nanopore data set
 827 was subsampled to 160x depth of coverage. Each read was aligned against NCBI-nr
 828 protein reference data base, then binned and visualized using Megan-LR.



829

830 **Supplementary Figure 10. Megan taxonomic read distribution at different ranks**
 831 **obtained from HM-276 PacBio sequenced data set.** HM-276D PacBio data set was
 832 subsampled to 160x depth of coverage. Each read was aligned against NCBI-nr protein
 833 reference data base, then binned and visualized using Megan-LR.

834



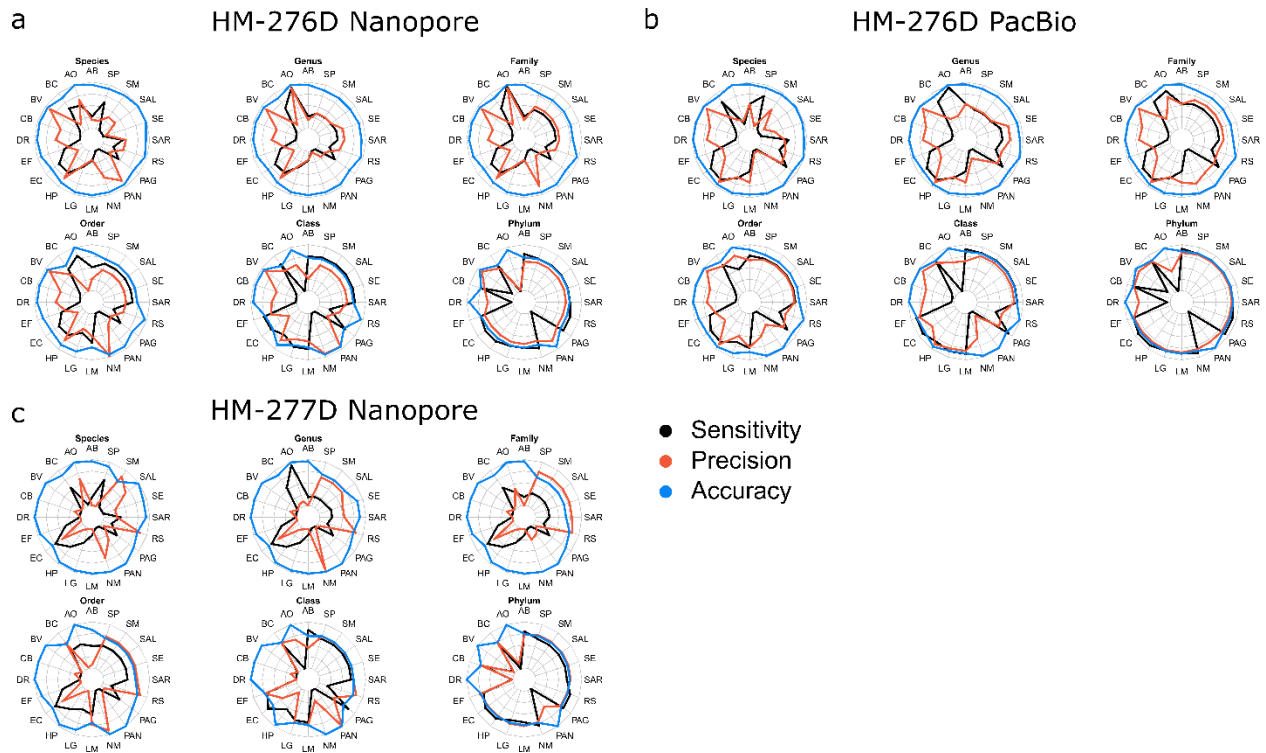
835

836 **Supplementary Figure 11. Strain-specific read assignment performance**
837 **comparison across sequencing technologies.** Read assignment accuracy statistics
838 for each bacterial strain were summarized based on datasets: HM-276D Nanopore **(a)**,
839 HM-276D PacBio **(b)** and HM-277D Nanopore **(c)** across ranks. Colors indicates different
840 metrics: sensitivity, precision and accuracy. Taxon were accurately recovered above the
841 family level. HM-276D Nanopore outperformed other two data sets. AB, *Acinetobacter*
842 *baumannii*; AO, *Actinomyces odontolyticus*; BC, *Bacillus cereus*; BV, *Bacteroides*
843 *vulgatus*; CB, *Clostridium beijerinckii*; DR, *Deinococcus radiodurans*; DF, *Enterococcus*
844 *faecalis*; EC, *Escherichia coli*; HP, *Helicobacter pylori*; LG, *Lactobacillus gasseri*; LM,
845 *Listeria monocytogenes*; NM, *Neisseria meningitides*; PAN, *Propionibacterium acnes*;
846 PAG, *Pseudomonas aeruginosa*; RS, *Rhodobacter sphaeroides*; SAR, *Staphylococcus*
847 *aureus*; SE, *Staphylococcus epidermidis*; SAL, *Streptococcus agalactiae*; SM,
848 *Streptococcus mutans*; SP, *Streptococcus pneumoniae*.

849

850

851



852

853 **Supplementary Figure 12. Strain-specific base pair assignment performance**
854 **comparison across sequencing technologies.** Read base assignment accuracy
855 statistics for each bacterial strain were summarized based on datasets: HM-276D
856 Nanopore **(a)**, HM-276D PacBio **(b)** and HM-277D Nanopore **(c)** across ranks. Colors
857 indicates different metrics: sensitivity, precision and accuracy. PacBio performed better
858 than Nanopore data above the family level because of lower error rate. AB, *Acinetobacter*
859 *baumannii*; AO, *Actinomyces odontolyticus*; BC, *Bacillus cereus*; BV, *Bacteroides*
860 *vulgatus*; CB, *Clostridium beijerinckii*; DR, *Deinococcus radiodurans*; DF, *Enterococcus*
861 *faecalis*; EC, *Escherichia coli*; HP, *Helicobacter pylori*; LG, *Lactobacillus gasseri*; LM,
862 *Listeria monocytogenes*; NM, *Neisseria meningitides*; PAN, *Propionibacterium acnes*;
863 PAG, *Pseudomonas aeruginosa*; RS, *Rhodobacter sphaeroides*; SAR, *Staphylococcus*
864 *aureus*; SE, *Staphylococcus epidermidis*; SAL, *Streptococcus agalactiae*; SM,
865 *Streptococcus mutans*; SP, *Streptococcus pneumoniae*.

866

867